The Role of Conical Intersections in Non-Adiabatic and Topological Effects

Ph.D thesis

Tamás Vértesi

Department of Theoretical Physics
University of Debrecen
Debrecen, 2004

Ezen értekezést a Debreceni Egyetem TTK Fizika Doktori Iskola Atom- és molekulafizika programja keretében készítettem 2001-2004 között és ezúton benyújtom a Debreceni Egyetem TTK doktori (Ph.D.) fokozatának elnyerése céljából.

Debrecen, 2004. szeptember

Vértesi Tamás

Tanúsítom, hogy Vértesi Tamás doktorjelölt 2001-2004 között a fent megnevezett Doktori Iskola Atom- és molekulafizika programjának keretében irányításommal végezte munkáját. Az értekezésben foglaltak a jelölt önálló munkáján alapulnak, az eredményekhez önálló alkotó tevékenységével meghatározóan hozzájárult. Az értekezés elfogadását javaslom.

Debrecen, 2004. szeptember

Dr. Vibók Ágnes
témavezető

List of publications

This thesis is based on the following papers, which will be referred to in the text by their Roman numerals:

I **Ab initio conical intersections for the Na+H_2 system: A four-state study**
Á. Vibók, GJ. Halász, T. Vértesi, S. Suhai, M. Baer, JP. Toennies,
J. Chem. Phys., **119** (2003), 6588-6596.

II **The electronic non-adiabatic coupling matrix: A numerical study of the curl condition and the quantization condition employing the Mathieu equation**
T. Vértesi, Á. Vibók, GJ. Halász, A. Yahalom, R. Englman, M. Baer,
J. Phys. Chem. A., **107** (2003), 7189-7196.

III **On diabatization and the topological D-matrix: Theory and numerical studies of the H+ H_2 system and the C_2H_2 molecule**
M. Baer, T. Vértesi, Á. Vibók, GJ. Halász, S. Suhai,
Faraday Discuss., **127** (2004), 337-353.

IV **Derivation of the electronic nonadiabatic coupling field in molecular systems: An algebraic-vectorial approach**
T. Vértesi, Á. Vibók, GJ. Halász, M. Baer,
J. Chem. Phys., **120** (2004), 8420-8424.

V **An algebraic-vectorial approach to obtain molecular fields from conical intersections: numerical applications to H+H_2 and Na+H_2**
Á. Vibók, T. Vértesi, E. Bene, GJ. Halász, M. Baer,
submitted to J. Phys. Chem. A. (accepted)

VI **A field theoretical approach to calculate electronic Born-Oppenheimer coupling terms**
T. Vértesi, Á. Vibók, GJ. Halász. M. Baer,
J. Chem. Phys., **121** (2004), 4000-4013.

VII **On the peculiarities of the diabatic framework: new insight**
T. Vértesi, Á. Vibók, GJ. Halász, M. Baer,
J. Chem. Phys. , **120** (2004), 2565-2574.

VIII **Pair-annihilation of conical intersections and a study to infer the phenomenon**
T. Vértesi, E. Bene,
Chem. Phys. Lett., **392** (2004), 17-22.

IX **The Berry phase revisited: application to Born-Oppenheimer molecular systems**
T. Vértesi, Á. Vibók, GJ. Halász, M. Baer,
submitted to J. Phys. B.

X **The electronic diabatic framework: restrictions due to quantization of the non-adiabatic coupling matrix**
M. Baer, T. Vértesi, GJ. Halász, Á. Vibók,
submitted to J. Phys. Chem. A. (accepted)

Posters

A vector-field theoretical approach to calculate the molecular field created by non-adiabatic coupling terms
T. Vértesi, E. Bene, Á. Vibók, G. J. Halász, and M. Baer,
Faraday Discussions 127 Non-adiabatic effects in chemical dynamics, Oxford, UK, 5-7 April 2004.

Contents

Chapter 1

Introduction

Molecules are composed of fast moving light electrons and slow moving heavy nuclei. This fact was exploited by Born and Oppenheimer [1] who separated the motion of fast electrons and slow nuclei in a quantum mechanical framework. The Born-Oppenheimer (BO) adiabatic approximation represents one of the cornerstones of molecular physics and chemistry. It allows the calculation of dynamical processes in molecules to be divided into two stages. In the first stage, the electronic problem is solved keeping the atomic nuclei fixed in space. The calculation of electronic energies and wave functions for fixed nuclei has been developed to a high degree of sophistication and constitutes the core of modern quantum chemistry. In the second stage, the nuclear dynamics on a given predetermined electronic potential energy surface (PES) is treated. The BO approximation is frequently accurate enough to allow the detailed understanding and prediction of molecular properties and processes.
Another class of important and interesting phenomena, which is the subject of the present thesis, is associated with dynamical processes that are not confined to a single electronic surface. The BO approximation [1,2] is based on the fact that the spacings of electronic eigenvalues are generally large compared to typical spacings associated with nuclear motion. When this condition is violated, the so-called non-adiabatic coupling terms (NACTs) cause transitions between the adiabatic electronic states. In this case the fast-moving electrons can create exceptionally large forces, causing the nuclei to be strongly accelerated so that their velocities are no longer negligibly small. Thus the NACTs allow for the motion of nuclei to move on coupled multiple adiabatic electronic states. In this case in order to carry out an accurate treatment of the nuclear dynamics of the system, we must replace the ordinary BO approximation with the Born-Huang expansion [2], in which an arbitrary number of electronic states can be included.

Their are a large class of chemically interesting processes, where the use of the Born-Huang coupled nuclear motion Schrödinger equations are justified, include for instance most of the photochemical reactions in the nature (i.e. photodissociation in which a molecule breaks up after absorbing a photon, or bound state photoabsorption when there is no reaction).

Indeed, at the exact position of degeneracy the energy gap between two adjacent electronic states becomes zero and the NACTs consequently may become infinitely large. Therefore molecular systems exhibiting degeneracies especially require the multi-state Born-Huang treatment. For a polyatomic system involving N atoms, where N≥3 (i.e. for not diatomic molecules), any two adjacent adiabatic electronic states can be degenerate for a set of nuclear geometries even if those electronic states have the same symmetry [3]. These intersections occur more frequently in such polyatomic systems [4] than it was previously believed. The reason is that these systems possess three or more internal nuclear motion degrees of freedom, and only two independent relations between three electronic Hamiltonian matrix elements (in a simple two electronic state picture) are sufficient for the existence of doubly degenerate energy eigenvalues. As a result, these relations can be easily satisfied explaining thereby the frequent occurrence of intersections [5-8]. If the lowest order terms in the expansion of these elements in displacement away from the intersection geometry are linear (as it is usually the case), these intersections are conical, the most common type of intersection [3,9]. Longuet-Higgins revealed an interesting topological fact related to a conical intersection (denoted by *ci*): assuming the adiabatic electronic wave functions of the two interesting states to be real and continuous as possible in nuclear coordinate space if the polyatomic system is transported around a closed loop in that space (a so-called pseudorotation) that encircles one conical intersection geometry, these electronic wave functions must change sign [3,10]. This change of sign requires the adiabatic nuclear wave functions to undergo a compensatory change of sign, known as the geometric phase (GP) effect [11-14] to keep the total wave function to be singe valued. Longuet-Higgins' findings were not just curiosities, they have profound effect on nuclear dynamics as was first pointed out by Mead and Truhlar [13]. They introduced a vector potential in the nuclear Schrödinger equation (SE) in order to ensure a single valued and continuous total wave function. Since the effect was analogous to that of Aharonov and Bohm (AB) [15], the name „molecular Aharonov-Bohm effect" (MAB) [13,16] was proposed for this phenomenon. Kupperman and co-workers identified this GP effect for the first time in a chemical reaction [17]. Their theoretically calculated integral cross-sections agreed well with experimental data at different energies [18]. The nuclear SE equation however, which describes well the MAB effect, essentially remains a single-state Schrödinger equation, thus it can not account for transitions between the electronic states, i.e. does not interpret well the so-called non-adiabatic effects. Therefore we expect that in

order the solution for high energy processes to be correct, the nuclear SE equations should include more excited states as well.

Briefly we can say that a conical intersection has a double role in chemical processes: on one hand it imposes a given boundary condition on the nuclear wave function (i.e. causing the GP effect), but on the other hand it couples adjacent electronic states, thereby allowing the system to evolve non-adiabatically, that is, in more than one electronic states. Certainly, as we have written above, this last feature can not be treated within the MAB theory, it needs a rigorous quantum formalism, the Born-Huang expansion, to treat the polyatomic systems properly.

The Born-Huang picture is based on two basic concepts: the PESs and the NACTs, and as we have seen these later coupling terms are spiky functions of the coordinates (it has a pole in the exact point of degeneracy [19,20]), therefore they cause numerical instabilities when solution of the corresponding nuclear SE is attempted. The only way to overcome this numerical difficulty is to move from the adiabatic Born-Huang framework to a diabatic one, where the NACTs are replaced by potential coupling terms that are smooth functions of the coordinates [21,22]. It can be achieved by a unitary transformation called the adiabatic-to-diabatic transformation (ADT) matrix [23]. Baer suggested the derivation of the ADT matrix for a tri-atom system by solving an integral equation along a two-dimensional contour [24], in addition, sufficient conditions were derived for the existence of the solution, which are termed the 'curl-conditions'. Recently, it has been proven that in order to produce a uniquely defined diabatic potential matrix (the matrix of the diabatic framework) from the NACTs, the ADT matrix has to fulfill quantization-type requirements [25]. Both of the above conditions (the quantization and the curl) are fulfilled when the eigenfunctions of the Born-Huang equations span a full Hilbert space [24,25].

Summing up we can claim, that any molecular system which exhibits conical intersection (which is not very rare, as it was revealed due to numerous ab-initio calculations and presented e.g. for two systems in Chapter 2) and is involved in non-adiabatic process, needs the diabatic framework for the proper quantum mechanical treatment. In this way the ADT matrix has a key role in any non-adiabatic process. In order to have an exact solution for the ADT (and the existence of a strictly diabatic representation) all possible adiabatic states should be included. Certainly it can not be accomplished as it would imply an infinite dimensional ADT matrix, but the question arises whether we can relax the conditions and thereby substantially decrease the number of states (to

N=2…5) to form a Hilbert subspace with a good approximation in a given region of our interest.

We note that throughout the thesis we do not use the conventional meaning of the Hilbert subspace. We use it in the case, when a group of states is strongly coupled to itself and, at most, weakly coupled to other states belonging to this manifold (in the region of interest), that is they are isolated well from "the rest of the world".

In Chapter 3 we represent very promising results about the possibility of reducing the complete Hilbert space to a finite Hilbert subspace, both by choosing a model system (based on the eigenfunctions of the Mathieu equations) and a real molecular system ($H+H_2$) for our numerical study. Since conical intersection lies in the confluence of two adjacent PESs, it has a dominant role in coupling these consecutive states, and therefore we expect that these states must be involved in the Hilbert subspace. The results will support our expectations and the 'quality' of the corresponding Hilbert subspaces will be tested both by the curl and quantization conditions.

However, by making friendly in size the ADT matrix we also need to gain from ab-inito calculations all the relevant NACTs in the whole configuration space (CS) of our interest in order to form the ADT matrix. Although nowadays their exist standard quantum chemistry computer packages, such as MOLPRO [26], and COLUMBUS [27,28] which calculate non-adiabatic coupling terms, it is still a very time consuming task, therefore our intention was to represent a model in Chapter 4 based on either a simple vector algebra or on certain field equations to be solved, in order to obtain the NACTs in every desired point of the nuclear configuration space. In the heart of the model lies the assumption that the NACTs behave like ordinary vector fields created by sources which have the positions of conical intersections (where NACTs become singular). The vector-algebraic model is worked out for the two-state Hilbert subspace, while the model generated by the field equations is an extension to the three-state case.

Since we found in Chapter 3 that the number of N states which forms a Hilbert subspace in a quite large region of CS could be N=2 with a good quality (especially when all the degeneracies are coupling the same two adjacent states) we felt interesting to study in Chapter 5 theoretically the diabatic representation of a two-state system with the aim of earning insight regarding the distribution of conical intersections in this region of CS. In this process we revealed explicit relationship between the diabatic potentials and the locations of conical intersections. The study is accompanied with numerical examples as worked out for the ab-initio potential energy surfaces of the $Na+H_2$ system. The results

are very useful, since the positions and number of *ci*s in a given region has a great importance in any non-adiabatic process. This method can be considered as a generalization of Longuet-Higgins' topological test for intersections [10], since our new method exhausts more topological information associated with the behavior of the eigenvectors concerning the presence of degeneracies. However, we have to note that our method in its present form can be applied only for a two-level system, while Longuet-Higgins' method is applicable for system with any dimension of Hilbert space.

In Chapters 2-5 we mostly deal with problems concerning the time-independent framework of the Born-Huang equations to study the NACTs, the ADT matrix and the diabatic potentials in order to infer some essential features of the above matrices regarding to the exact description of non-adiabatic processes. In Chapter 6, however we analyze molecular systems from an other point of view, namely via a semi-classical framework: we assume that one of the nuclear components of the molecular system is guided by an external potential of the electromagnetic field. This potential forces the two parts of the molecule to revolve with respect to one an other, and thus inducing transitions with some oscillating probabilities to other states regarded to the initial one. The above description of the situation is exactly the context where the use of Berry's phase [14] is justified: "The phase that can be acquired by a state moving adiabatically (slowly) around a closed path in the parameter space of the system". Macroscopic physical manifestations of this type of situation from other area of physics may be found in the Aharonov-Bohm effect [15], or in nuclear magnetic resonance (NMR) systems subject to slowly rotating magnetic fields [29], or it has been investigated for neutron spin [30] and photons [31], as well. In Chapter 6 we study the implementation of the Berry approach [14] within the Born-Oppenheimer molecular systems as we described it previously. We reveal relation between the Berry phase and the elements of the final ADT-matrix (at the end of the closed trip in the configuration space) in the adiabatic limit. Based upon Pancharatnam's work [32], who has introduced already in 1956 the concept of geometric phase in his studies of interference effects of polarized light waves, Samuel and Bhandari [33] introduced the notion of open-path geometric phases, which phase can be applied for a non-cyclic and non-adiabatic evolution. We extend the study to deal with this situation as well, and will find further interesting connections between the open-path phase and the elements of the ADT. This theoretical study will be supported by a detailed numerical study carried out for the ($Na+H_2$) system.

The plan of this thesis is as follows.

In Chapter 2 we introduce the Born-Huang formalism together with a brief theoretical background of the non-adiabatic coupling terms. We also represent the two molecular systems ($Na+H_2$) and ($H+H_2$), which are subject of the numerical studies.

Chapter 3 is devoted to the subject that in what extent the relevant group of states forms a Hilbert subspace in a polyatomic system in a given region of configuration space.

In Chapter 4 we develop a model to calculate the non-adiabatic coupling terms, based either on a simple vector algebra in the two-state Hilbert subspace, or on the 'curl-divergency' field equations in the three-state Hilbert subspace.

In Chapter 5 a method is discussed which reveals explicit connection between the diabatic potentials and the locations of conical intersections.

In Chapter 6 we study the implementation of the geometric phase within Born-Oppenheimer molecular systems in a semi-classical framework.

A summary of the new results are presented in Chapter 7.

Chapter 2

The Theoretical and Numerical Background

In this chapter we give a brief overview of the theory of the non-adiabatic coupling terms (Sec. 2.1) and review (Sec. 2.2) the ab-initio treatment to obtain these terms. In addition we represent the ($Na+H_2$) and ($H+H_2$) molecular systems, which are the subject of the numerial studies in the forthcoming chapters.

2.1 Study of the non-adiabatic coupling terms

The starting point for the theory of molecular dynamics and the basis for most theoretical chemistry is the separation of the nuclear and electronic motion. In the standard, adiabatic Born-Huang [2] picture this leads to the concept of nuclei moving over PESs corresponding to the electronic states of a system.

In its Cartesian form, the Hamiltonian can be written

$$\hat{H}(r,R) = \hat{T}_n(R) + \hat{H}_{el}(R,r) \tag{2.1}$$

where $\hat{T}_n$ is the nuclear kinetic energy operator and can be written in terms of mass-scaled coordinates as $\hat{T}_n = \frac{-\hbar^2}{2m}\nabla^2$, where m is the mass of the system, $\hat{H}_{el}$ is the clamped nucleus electronic Hamiltonian which depends parametrically on the nuclear coordinates, and r,R stand for the electronic and nuclear coordinates, respectively.

Next we employ the BO expansion:

$$\Psi(R,r) = \sum_{i=1}^{N} \psi_i(R)\zeta_i(r \mid R), \tag{2.2}$$

where $\{\psi_i(R)\}_{i=1}^{N}$ are the nuclear wave functions and $\{|\zeta_i(R)\rangle\}_{i=1}^{N}$ are the electronic eigenfunctions of the electronic Hamiltonian:

$$\hat{H}_{el}(r \mid R)\zeta_i(r \mid R) = u_i(R)\zeta_i(r \mid R) \tag{2.3}$$

Inserting the expansion Eq. (2.2) into the Schrödinger equation (SE) Eq. (2.1) and after some algebraic manipulation of the resulting equation we arrive at the coupled equations of the Born-Huang system in a matrix form:

$$\frac{-\hbar^2}{2m}\nabla^2\boldsymbol{\Psi}+(\mathbf{u}-E)\boldsymbol{\Psi}-\frac{\hbar^2}{2m}\left(2\boldsymbol{\tau}\nabla+\boldsymbol{\tau}^{(2)}\right)\boldsymbol{\Psi}=0 \tag{2.4}$$

where $\boldsymbol{\Psi}$ is the column vector that contains nuclear functions $\{\psi_i(R)\}_{i=1}^{N}$, $\mathbf{u}$ is a diagonal matrix which contains the adiabatic potentials (PES), $\boldsymbol{\tau}$ is the non-adiabatic (vector) matrix (NACT) with elements: $\boldsymbol{\tau}_{ij}=\left\langle\zeta_i\middle|\nabla\zeta_j\right\rangle$, and $\boldsymbol{\tau}^{(2)}$ is the second order (scalar) matrix with elements $\tau_{ij}^{(2)}=\left\langle\zeta_i\middle|\nabla^2\zeta_j\right\rangle$. We note that throughout the thesis the terms $\boldsymbol{\tau}$ matrix and the NACT matrix will be used interchangeable expressing the same matrix.

It is important to emphasize that Eq. (2.4) is valid for any group of states. Next we consider a group of N states (out of an infinite Hilbert space). The breakup of the Hilbert space is done according to the criteria [34] $|\boldsymbol{\tau}_{ij}|\approx 0$ for $i\le N$; $j>M$. In other words the NACTs between states that belong to the group and those outside the group are all assumed to be negligibly small. If this breakup takes place at every point in a given region we say that the N states form a Hilbert subspace in this region.

If the group of states forms an isolated Hilbert subspace according to the above definition then, and only then, Eq. (2.4) takes a simple form [34]:

$$\frac{-\hbar^2}{2m}(\nabla+\boldsymbol{\tau})^2\boldsymbol{\Psi}+(\mathbf{u}-E)\boldsymbol{\Psi}=0\,, \tag{2.5}$$

where we used the fact that in case of a full orthonormal set of $\{|\zeta_i(R)\rangle\}_{i=1}^{N}$

$$\boldsymbol{\tau}^{(2)}=\boldsymbol{\tau}^2+\nabla\boldsymbol{\tau}\,. \tag{2.6}$$

The NACT matrix elements $\boldsymbol{\tau}_{ij}$ can be evaluated analytically with the knowledge of the $|\zeta_i(R)\rangle$ adiabatic electronic eigenfunctions, using an off-diagonal form of the Hellmann-Feynman theorem [35-37]

$$\frac{\partial\left\langle\zeta_i\middle|\hat{H}_{el}\middle|\zeta_j\right\rangle}{\partial R}=\left\langle\zeta_i\middle|\hat{H}_{el}\middle|\frac{\partial\zeta_j}{\partial R}\right\rangle+\left\langle\frac{\partial\zeta_i}{\partial R}\middle|\hat{H}_{el}\middle|\zeta_j\right\rangle+\left\langle\zeta_i\middle|\frac{\partial\hat{H}_{el}}{\partial R}\middle|\zeta_j\right\rangle. \tag{2.7}$$

As $\{|\zeta_i(R)\rangle\}_{i=1}^{N}$ are eigenvectors of $\hat{H}_{el}$ at all values of R, the lhs. of Eq. (2.7) reduces to zero (when $i\neq j$), and finally with some algebraic operations we obtain

$$\boldsymbol{\tau}_{ij}=\frac{1}{u_j-u_i}\left\langle\zeta_i\middle|\frac{\partial\hat{H}_{el}}{\partial R}\middle|\zeta_j\right\rangle. \tag{2.8}$$

Thus it is well noticed that when the *i*th and *i+1*th eigenvalues (between two consequtive pairs) become degenerate the corresponding $\boldsymbol{\tau}$ matrix element i.e. $\boldsymbol{\tau}_{i,i+1}$ becomes singular. However, we have to realize that for molecular systems that contain singular NACTs, Eq. (2.5) can not be solved because of the non-analytic feature of the NACTs and therefore is of no practical use. Eq. (2.5) is known as the nuclear SE within the adiabatic framework. Now our aim is to eliminate the unpleasant singular NACTs from Eq. (2.5) by transforming to the diabatic framework, and for this purpose we perform the following transformation:

$$\boldsymbol{\Psi} = \mathbf{A}\boldsymbol{\Phi}\,, \tag{2.9}$$

The matrix **A** is termed the adiabatic-to-diabatic transformation (ADT) matrix, because of its fundamental role in transforming between the two frameworks. Our next step is to obtain the **A** matrix, which is yet undetermined. Substituting Eq. (2.9) into Eq. (2.5) then performing the usual algebra, and demanding the elimination of the $\boldsymbol{\tau}$ matrix, yields the following results:

The new, diabatic SE is

$$\frac{-\hbar^2}{2m}\nabla^2\boldsymbol{\Phi} + (\mathbf{W} - E)\boldsymbol{\Phi} = 0\,, \tag{2.10a}$$

and the corresponding diabatic Hamiltonian is

$$\hat{H}_{dia} = \hat{T}_N + \mathbf{W}\,, \tag{2.10b}$$

where the diabatic potential is given in the following form:

$$\mathbf{W} = \mathbf{A}^{\mathrm{T}}\mathbf{u}\mathbf{A}\,, \tag{2.11}$$

and the matrix **A** is a solution of the following first order differential equation:

$$\nabla\mathbf{A} + \boldsymbol{\tau}\mathbf{A} = \mathbf{0} \tag{2.12}$$

In order to have a solution for the ADT matrix in Eq. (2.12), it is a sufficient condition for **A** to be analytic, which implies that the 'curl condition' has to be fulfilled for the NACTs [24]: Introduce the matrix **F**, defined as

$$F_{pq} = \frac{\partial \tau_p}{\partial q} - \frac{\partial \tau_q}{\partial \tau_p} - \left[\tau_p, \tau_q\right], \tag{2.13}$$

where *p* and *q* are two nuclear Cartesian coordinates, in the case the group of states forms an isolated Hilbert subspace, according to the 'curl condition' **F**=0 must be satisfied at every point in the configuration space. Writing **F** in a more compact way, this means

$$\mathbf{F} = curl\boldsymbol{\tau} - \left[\boldsymbol{\tau} \times \boldsymbol{\tau}\right] = 0\,. \tag{2.14}$$

In summary we can say, that the adiabatic framework (described by Eq. (2.5)) is the standard one in quantum chemistry for the reason, that it is the one which is used in ab-initio calculations, i.e. which solves the electronic

Hamiltonian at a particular nuclear geometry. In this case the full information about the nuclear dynamics is carried by the adiabatic potential energy surfaces (i.e. the **u** matrix) and the non-adiabatic coupling operator matrix (i.e the **τ** matrix). However, in the diabatic framework (defined by Eq. (2.10a-b)) the electronic wave functions are no longer eigenfunctions of the electronic Hamiltonian. The aim is instead that the functions are so chosen that the nonlocal **τ** matrix elements, and the couplings are represented by local potential operators, the so-called diabatic potential matrix **W**.

Since the elements of the diabatic PES matrix are smooth functions of the coordinates in contrast to the NACTs, the diabatic framework is preferred for treating the nuclear dynamics of the nuclei, and all rigorous quantum-mechanical treatments aim at reaching it.

An elegant way to gain the diabatic potential **W** can be accomplished through Eq. (2.11). In this indirect way we derive for each point in the configuration space the adiabatic electronic eigenfunctions to calculate the NACTs and the corresponding electronic eigenvalues. Then with the knowledge of **τ** we solve Eq. (2.12) for the matrix **A**, and substitution to Eq. (2.11) yields the diabatic potential **W**. In order to calculate **A** at a given point R, we have to assume a contour Γ that connects the point R and the starting point R_0, and solve Eq. (2.12) along this contour. The solution is given in the form [38]:

$$\mathbf{A}(R,R_0)=\hat{P}\exp\left(-\int_{R_0}^{R}\boldsymbol{\tau}dR\right)\mathbf{A}(R_0), \tag{2.15}$$

where $\hat{P}$ is the path ordering operator, and $\mathbf{A}(R_0)$ is a matrix that contains boundary values. Closing the contour in Eq. (2.15) leads to the matrix $\mathbf{D}(\Gamma)$, namely

$$A(R=R_0,R_0)=D(\Gamma)=\hat{P}\exp\left(-\oint_{\Gamma}\boldsymbol{\tau}dR\right). \tag{2.16}$$

Now our aim is to find a connection between the elements of the matrix $\mathbf{D}(\Gamma)$ and the electronic eigenfunctions which are parallel transported on the particular closed contour Γ. To form the connection between two nearby Hilbert spaces we consider the kth electronic ket $|\zeta_k(R)\rangle$ (defined by Eq. (2.3)) at the point $R+\Delta R$:

$$|\zeta_k(R+\Delta R)\rangle=\sum_{i=1}^{N}|\zeta_k(R)\rangle(\delta_{ki}+\Delta R\boldsymbol{\tau}_{ik}). \tag{2.17}$$

The previous equation is merely a first order expansion in R and is always fulfilled if the set $\{|\zeta_k(R)\rangle\}_{i=1}^{N}$ forms a complete basis. Using Eq. (2.17) we can write in general a displacement of the basis at R_0 to R:

$$|\zeta_k(R)\rangle = \sum_{m=1}^{N} \mathbf{A}^*(R,R_0)_{km} |\zeta_m(R_0)\rangle, \tag{2.18}$$

where the numerical matrix is defined by

$$\mathbf{A}^*(R,R_0) = \hat{P}\exp\left(-\int_{R_0}^{R} \boldsymbol{\tau} dR\right). \tag{2.19}$$

Comparing the expression for $\mathbf{A}^*(R,R_0)$ in the above equation with the expression for $\mathbf{A}(R,R_0)$ in Eq. (2.15), we can realize that choosing as a boundary $\mathbf{A}(R_0) = I$ in Eq. (2.15) entails

$$\mathbf{A}^*(R,R_0) = \mathbf{A}(R,R_0). \tag{2.20}$$

Thus closing the contour, and applying Eq. (2.18) leads to

$$\zeta(r \mid R_0 \mid \Gamma) = \mathbf{D}(\Gamma)\zeta(r \mid R_0), \tag{2.21}$$

where ζ denotes the vector formed by $\{|\zeta_k\rangle\}_{i=1}^{N}$, and Γ is the particular closed contour. This **D**-matrix plays an important role in the theory because it contains all topological features of an electronic manifold in a region surrounded by the contour Γ as it can be inferred from the definition contained by Eq. (2.21):
the **D**-matrix is diagonal and has in its diagonal numbers of norm 1. Since we consider only real electronic eigenfunctions these numbers can be either (+1)s or (-1)s. Moreover, the positions of the (-1)s are associated with the electronic eigenfunctions that flip their sign.

Let us simplify our treatment and examine the two-state case. For a system of real Hamiltonian $\boldsymbol{\tau}$ is a real, antisymmetric matrix, thus in the two-state case the NACT matrix has one nonzero term $\boldsymbol{\tau}_{12}$=$\boldsymbol{\tau}_{21}$, and for this case one can evaluate analytically the ordered exponential in Eq. (2.16), and yields the following **D**-matrix [39]:

$$D = \begin{pmatrix} \cos\oint_{\Gamma} \boldsymbol{\tau}_{12}(R)dR & \sin\oint_{\Gamma} \boldsymbol{\tau}_{12}(R)dR \\ -\sin\oint_{\Gamma} \boldsymbol{\tau}_{12}(R)dR & \cos\oint_{\Gamma} \boldsymbol{\tau}_{12}(R)dR \end{pmatrix} \tag{2.22}$$

Next we refer to the requirements to be fulfilled by the matrix **D**, that it is diagonal and that it has in the diagonal numbers which are of norm 1. In order for that happen the vector function $\boldsymbol{\tau}_{21}$(R) has to fulfill along a given closed path Γ the condition [25,39]:

$$\oint \boldsymbol{\tau}_{12}(R) dR = n\pi , \tag{2.23}$$

where n is an integer. Eq. (2.23) is a quantization condition on the matrix element $\boldsymbol{\tau}_{12}$. We note that this condition must be always fulfilled whenever the dimension of Hilbert subspace in the region encircled by the contour Γ can be considered N=2. However, excluding singularities of the NACTs the curl condition for two-state case in Eq. (2.14) becomes $curl\boldsymbol{\tau}_{12} = 0$, which entails, by applying Stokes' theorem, that as a special case n=0 in Eq. (2.23).

2.2 Numerical details of $H+H_2$ and $Na+H_2$

In the preceding section the theory required to study non-adiabatic effects on molecular systems has been outlined. Now, we give a brief overview in subsection (2.2.1) about the details of the ab-initio treatments, and discuss in subsection (2.2.2) the positions of the various conical intersections in the two tri-atomic systems the $H+H_2$ and $Na+H_2$ under investigation.

2.2.1 The ab-initio calculations

At present the best general methods for the treatment of polyatomic molecules are the MCSCF methods, of which the CASSCF method is particularly powerful. The MCSCF methods describe a wave function by a linear combination of M configuration state functions (CSFs), Φ_k, with CI coefficients, C_k,

$$\zeta(r) = \sum_{k=1}^{M} C_k \Phi_k . \tag{2.24}$$

In practice each CSF is a Slater determinant of molecular orbitals, which are divided into three types: inactive (doubly occupied), virtual (unoccupied), and active (variable occupancy). The active orbitals are used to build up the various CSFs, and so introduce flexibility into the wave function by including configurations that can describe different situations. Approximate electronic wave functions are then provided by the eigenfunctions of the electronic Hamiltonian in the CSF basis. This contrasts to the standard HF theory in which only a single determinant is used without active orbitals. The MCSCF method then optimizes both the molecular orbitals, represented as usual in SCF calculations by linear combinations of atomic orbitals (LCAO), and the CI expansion coefficients to obtain the variational wave function for one state. The optimization of the orbitals for a particular state, however, will not converge if

a degeneracy, or a near degeneracy of states is present, as the wave function will have problems following a single state. To overcome this, state-averaged orbitals (SA-MCSCF) must be used [40,41]. In this case rather than optimizing a single eigenvalue of the Hamiltonian matrix, an averaged energy function is used so that the orbitals describe all the states of interest simultaneously to the same accuracy. The strength and weakness of the method comes from the fact that the orbitals involved in a particular process must be selected and included in the captive space. Only the important orbitals are used, so accurate calculations can be made relatively cheaply. If the active space is however, badly chosen, this may lead to qualitatively incorrect results due to imbalances in the basis set. Using MCSCF methods it is also possible to obtain the non-adiabatic coupling terms using analytic procedures [41]. SA-MCSCF must again be used in the calculation of the NACTs, as the functions for the two states must be described to the same level of accuracy.

In the actual calculations the non-adiabatic coupling terms were calculated employing the analytical gradient technique of the MOLPRO [40] program for state averaged CASSCF wave functions. In both systems ($H+H_2$ and $Na+H_2$) the ab-initio calculations were carried out at the state-averaged CASSCF level with the 6-311G** basis set.

(i) In the $H+H_2$ system the basis set was extended with additional diffuse functions. In order properly to take into account the Rydberg states it was added to the basis set one s and one p diffuse function in an even tempered manner, with exponents of 0.0121424 and 0.046875, respectively. The active space included all three electrons distributed over nine orbitals. Usually five different electronic states (depending on the case), namely, 1 ^{2}A', 2 ^{2}A', 3 ^{2}A', 4 ^{2}A' and 5 ^{2}A' were computed by the state-averaged CASSCF method with equal weights.

(ii) In the $Na+H_2$ system we used the active space including all three valence electrons distributed on 16 orbitals. Seven electronic states, including the four studied states were computed with equal weights.

2.2.2 Revealing the position of conical intersections

Now we are particularly interested in both molecular systems of the position of the conical intersections (*ci*s), i.e. the points in the two-dimensional configuration space where at least two adjacent states (j) and (j+1) become degenerate. In order to reveal the position of *ci*s in an unexplored system we have to allow only two nuclear coordinates to be varied, and the rest must be

frozen (unless the *ci*s are not points but higher dimensional objects). Throughout this work we merely deal with tri-atomic molecular systems, and the nuclear configuration space we treat is formed by fixing the distances of two (out of three) atoms and let the third atom move freely on this surface of CS. Thus the third atom determines a plane with polar coordinates (q,φ) which at the same time serves as a test-particle to search for *ci*s. These conical intersections can be explored on several ways, below we give a list of them:

(a) It can be called direct way [5], since *ci*s are found by tracing the energy gaps between particular states, and in this way assigning the points at which two (or more) adiabatic states (surfaces) become degenerate. This method may miss an existing *ci* or define a situation of an "almost" degeneracy, as a *ci*, due to the numerical inaccuracy in computing the potential energy surfaces.

The other methods are called topological ones, since we exploit the topological nature of the *ci*s:

(b) It was pointed out by Longuet-Higgins et al. that when an electronic wave function is parallel-transported along a closed path around a conical intersection of a PES, the sign of the wave function is changed [3]. Longuet-Higgins also proved that when an electronic wave function changes sign after a circular transportation along a loop in the atomic configuration space, there must be a conical intersection within the loop [10]. We apply this theorem here to locate conical intersections via inspecting the diagonal elements of the topological **D**-matrix. Since we noticed in section (2.1) that the possible -1/+1 values are directly associated with the adiabatic eigenfunctions flipping/non-flipping signs when traversing the contour Γ, we can state that when denoting with n_j the number of *ci*s involving state j contained in the closed loop Γ entails that

$$\mathbf{D}_{jj} = (-1)^{n_j} \tag{2.25}$$

This method requires a group of N states (denoting by N the dimension of the **D**-matrix) isolated from the rest, i.e. the number of N states must form a Hilbert subspace, otherwise the diagonal elements of **D** will be not exactly ±1. Certainly this method can be applied as well when $\mathbf{D}_{ii} = \pm 1$ only with a good approximation, which usually can be guaranteed in many circumstances, for instance by increasing the number of states to form the **D**-matrix (a topic which will be accounted for in Chapter 3). A drawback of the Longuet-Higgins' topological approach related to search for intersections in a given region, that when each state involves even number of *ci*s, according to Eq. (2.25) the method is not capable to signal degeneracies inside the loop.

(c) The problem with the above method can be partialy circumvented by observing the off-diagonal form of the Hellmann-Feynman theorem in Eq. (2.8). In the case of a conical degeneracy between states j and j+1 the numerator in Eq. (2.8) is nonvanishing thus the element $\boldsymbol{\tau}_{jj+1}$ has a pole. This means (using first order perturbation theroy) that close to the intersection $\left|\boldsymbol{\tau}_{jj+1}\right| \propto \frac{1}{r}$, where r denotes the distance from the point of intersection. Therefore in our case when the test particle, namely the Hydrogen atom is relatively close to the degenerate point (between j and j+1 states) the amplitude of the corresponding $\boldsymbol{\tau}_{jj+1}$ element becomes very large indicating a degeneracy in the neighborhood of the moving Hydrogen's actual position.

Summing up the features of the above (a)-(c) methods we can notice that in a real situation when there is no previous information about the topology of *ci*s in a molecular system, the best working method seams to be a combination of the above mentioned ones.

In the following we describe the revealed *ci*s in each molecular system. We introduce a new notation by designating a *ci* between the j and j+1 states as (j,j+1) *ci*. The following findings about the position of the various *ci*s of the $H+H_2$ and $Na+H_2$ systems have been revealed in subsequent publications of Ref. [5,7] and paper **I**.

(i) The $H+H_2$ is characterized by the fact that its three lowest states namely, the $1^2A'$, the $2^2A'$ and the $3^2A'$ states are strongly coupled to each other. In general the type of coupling terms that dominate the interaction between the three states depends on the nuclear configuration [7]. Here we limit ourselves to a situation where two hydrogen atoms are at a (fixed) distance $R_{HH} = 0.74$ Å. In this situation the two lower states of the $H+H_2$ system are coupled by an *equilateral* (1,2) *ci*, labeled as a D_{3h} *ci* and the second and the third states are coupled by two C_{2v} *ci*s formed by the corresponding isosceles triangles. These two (2,3) *ci*s, sometimes termed as twin *ci*s, are located on the two sides of the line that combines the center-of-mass of the two bonded hydrogens and the third (loose) hydrogen (see the schematic geometry in Fig. 2.1a).

(ii) In the $Na+H_2$ we are interested again in a situation where the distance between the two hydrogens is fixed and in this case assumed to be 2.18 a.u. and the sodium is allowed to move freely (in the plane). In Fig. 2.1b are shown the positions of the various *ci*s. It was found in paper **I**. that the (1,2) *ci* is a C_{2v} *ci*

located on the symmetry line orthogonal to the HH axis, the (2,3) *ci*s are C_{2v} *ci*s located on the HH axis, and out of the four (3,4) *ci*s two of them are C_{2v} *ci*s located on the symmetry line orthogonal to the HH axis, at a distance of r~1.145a.u. and 1.580a.u. from the HH axis and two C_s twin *ci*s located on both sides of the just mentioned symmetry line at a distance of r = 1.533a.u. from the HH axis and at an angle of 12.2° off this symmetry line.

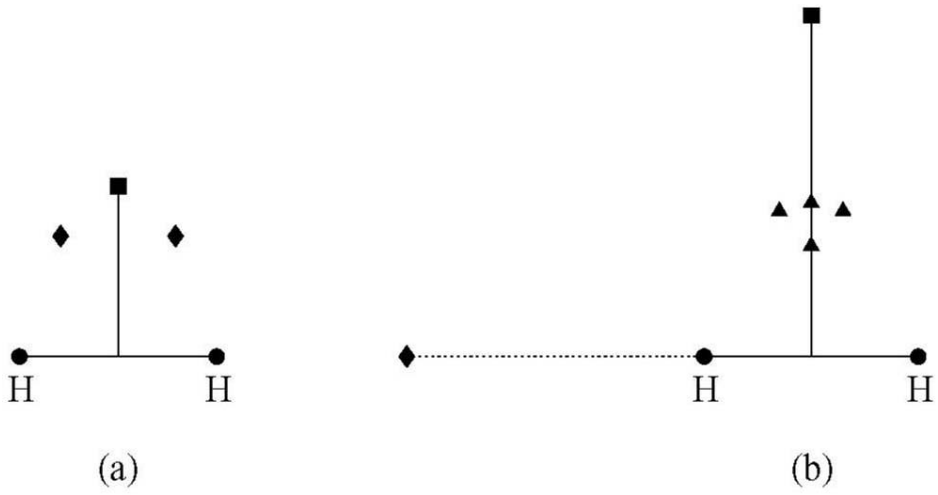

Figure 2.1: Positions of the various conical intersections: (1,2), (2,3) and (3,4) *ci*s are labeled with markers ■,♦,▲, respectively. Subfigure (a) shows the topology of the $H+H_2$ system, while (b) shows the $Na+H_2$ system

Chapter 3

The Quantization and the Curl Condition

In this chapter we study two features of the non-adiabatic coupling matrix $\boldsymbol{\tau}$, namely:

(i) its components fulfill the curl condition, ie. according to Eq. (2.14) the **F**-matrix is a zero matrix.

(ii) it is quantized in the sense that the **D**-matrix presented in Eq. (2.16) is an orthogonal diagonal matrix.

These conditions are satisfied when the group of states forms a complete Hilbert space. However the validity of these conditions can be extended for group of states which do not form a Hilbert space but in the region of interest are well isolated from "the rest of the world". The case (ii) can be derived from Eq. (2.17) as it is intuitively clear that Eq. (2.17) is valid only when all possible adiabatic states of the isolated Hilbert subspace are included.

It is known from perturbation theory [42] that a region surrounding a *ci* can always be made small enough so that the 2x2 **D**-matrix (see Eq. 2.22) is an orthogonal diagonal matrix which implies that the two relevant states form a Hilbert subspace in this small region [8,43]. However when we extend the region round the *ci*, the 2x2 **D**-matrix is no longer quantized (i.e. it does not fulfill (ii)), and we have to extend the number of states and add an other state to form a 3x3 **D**-matrix which will be quantized again. Thus it seems that the larger the region the more states are required in order to make the relevant **D**-matrix diagonal. Certainly we expect the same feature from the **F**-matrix, as well. This chapter and the corresponding **II** and **III** papers are devoted to this subject.

Section (3.1) is based on the paper **II**. We preview the main principles of the study concerning a model system based on the Mathieu equation. Then we discuss the feature (i) namely the fulfillment of the curl condition in subsection (3.1.1), and quantization condition (ii) in subsection (3.1.2). Section (3.2) is based upon paper **III**, which deals again with feature (ii), ie. the quantization condition for the **D**-matrix in the $H+H_2$ realistic system.

3.1 The model system

The idea was to consider for this purpose a simple model for which the 'electronic' eigenstates can be easily produced and particularly the following relations can be studied quantitatively: (1) for a given value of N (where N is the dimension of the matrix $\boldsymbol{\tau}$), increasing the region of configuration space $\boldsymbol{\Lambda}$ how the fulfillment of the above quantization and curl conditions are harmed); (2) to what extent the increase of N for a given region $\boldsymbol{\Lambda}$ improves the fulfillment of the above conditions.

Based on previous experiences [44,45] we chose for this task the Mathieu equation. This equation is characterized by one electronic coordinate (θ) and two nuclear coordinates (q,ϕ):

$$\left(-\frac{1}{2}E_{el}\frac{\partial^2}{\partial\theta^2}-kq\cos(2\theta-\phi)-u_j(q,\phi)\right)\zeta_j(\theta\,|\,q,\phi)=0\,. \qquad (3.1)$$

Here E_{el} is a characteristic electronic quantity, $u_j(q,\phi)$ and $\zeta_j(\theta|q,\phi)$ are the j-th eigenvalue and eigenfunction, respectively, which parametrically depend on the nuclear coordinates. The term, that couples the electronic and the nuclear motions and depends on all three of them, is written in the present application as a product $kq\cos(2\theta-\phi)$ which yields NACTs that are independent of the polar coordinate, ϕ - a fact which simplifies, significantly, the numerical treatment. Next we introduce a new parameter, *x* defined as:

$$x=q(k/E_{el}) \qquad (3.2)$$

In this notation the nuclear coordinate *x* is directly associated with the size of the region $\boldsymbol{\Lambda}$. Now we do not follow in detail on which way we solve Eq. (3.1) numerically, and how we obtain the NACTs and finally the two relevant matrix **F** and **D** (it is quite straightforward and can be find in the paper **II**). We merely show some final useful results coming from the treatment of the model.

3.1.1 Study of the D-matrix

The study of the **D**-dependence on x and N i.e. **D**(N,x), is presented in terms of the diagonal elements of the **D**-matrix, namely, $\mathbf{D}_{jj}$; {j=1,N}. Note, that since the matrix elements of $\boldsymbol{\tau}$ do not depend on ϕ, this also applies to the **D**-matrix. In the converged case (namely, the case for which the group of N states forms a Hilbert subspace in the circular region defined by x) we expect these diagonal

elements to be -1 for our particular model when N is an even number. Therefore, for a given N and x, a significant deviation of a diagonal term from -1 implies that within the region defined by x the considered N states do not form a Hilbert subspace. We observed in all cases, that the last diagonal element along the diagonal, namely, $\mathbf{D}_{NN}(N,x)$, shows, as x increases, the largest deviations from -1.0.

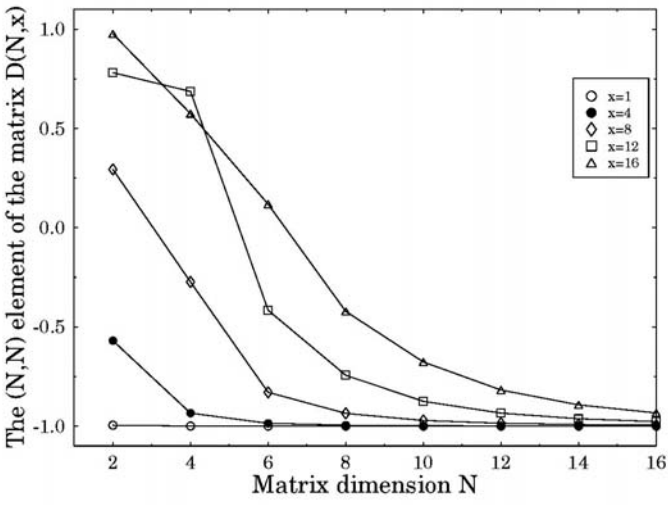

Figure 3.1: Highest diagonal elements $D_{jj}(N,x)$, calculated as functions of N for various x values.

Thus we present in Fig. 3.1 the $\mathbf{D}_{NN}(N,x)$-matrix elements as functions of N for different x-values. It is noticed that the various $\mathbf{D}_{NN}(N,x)$ curves decay asymptotically towards the value -1 as N increases but the rate of decay becomes slower the larger is x (i.e. the larger is the region in the configuration space). Thus it is noticed that e.g. at x=4 the rate of decay is very fast (all diagonal elements for $N \geq 4$ are already -1.0) but for x=16 the rate of decay is so slow that we reach the value of -1.0 only when $N \geq 16$. In summary, we showed here that the more extended is the region in the configuration space the larger is the required size of a set of states in order to be able to become a Hilbert subspace.

3.1.2 Study of the F-matrix

According to Eq. (2.14) the **F**-matrix can be written in the following form:

$$\mathbf{F} = curl\boldsymbol{\tau} - [\boldsymbol{\tau} \times \boldsymbol{\tau}]. \qquad (3.3)$$

With the aid of the numerically computed eigenfunctions $\zeta_j(\theta|q,\phi)$ we calculate the NACT terms and then produce the **F**-matrix elements as well. In Figs. 3.2 are presented the off-diagonal elements of the **F**–matrix (note the logarithmic scales along both axes): in Fig. 3.2a are shown the results for x=1 and in Fig. 3.2b for x=10. The interesting aspect of this study is the very fast decay of most of these matrix elements with N and the fact that they decrease to such small values as 10^{-10}. The only exception is the last off-diagonal element $\mathbf{F}_{N\text{-}1N}(x)$ which decreases with N but in a very slow rate.

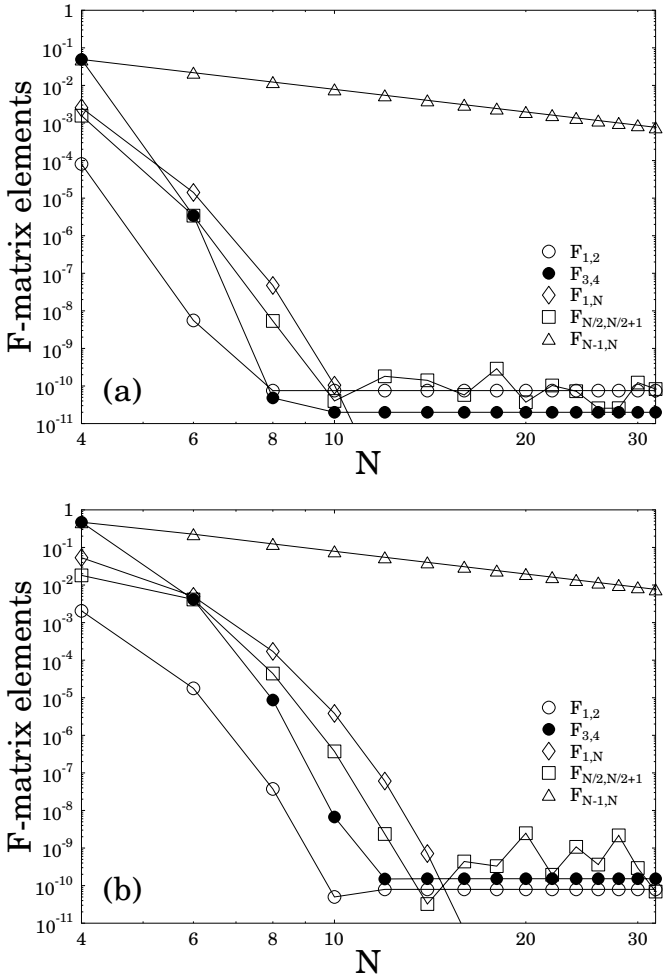

Figure 3.2: Off-diagonal matrix elements $\mathbf{F}_{jk}(N,x)$ calculated as a function of N for two x values. (a) x=1.0; (b) x=10.0.

Comparing the results for x=1 and x=10 it is noticed that in both cases the various values decrease to $\sim 10^{-10}$ but in case of x=1 the rate of decrease is faster. The reason is that it is easier for a given group of states to become a Hilbert subspace the smaller is the x-value, namely the smaller is the region surrounding the *ci*(s).

This feature is even better seen in Fig. 3.3 where are presented the same **F**–matrix elements but as a function of x calculated for a fixed value of N (=8). The results in this figure just support what is claimed in the previous paragraph namely that these matrix elements tend to increase as a function of x (when calculated for a fixed N-value).

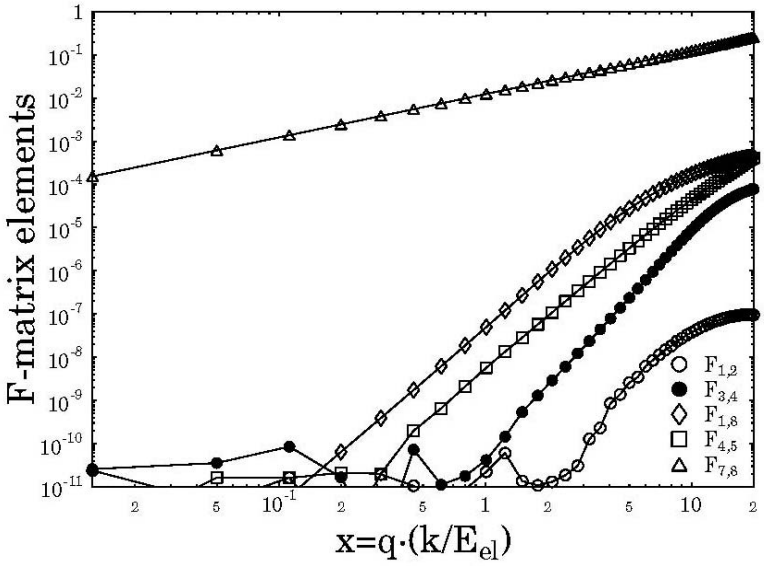

Figure 3.3: Off-diagonal matrix elements $\mathbf{F}_{jk}(N,x)$ calculated as a function of x for N=8.

In summary: we showed here (just as in the case of the study of the **D**-matrix) that the more extended is the region in the configuration space the larger is the required size of a set of states in order to be able to become a Hilbert subspace. In addition we found that the convergence toward a Hilbert subspace is relatively fast (both with respect to the analysis of the **D** and **F** matrices).

3.2 The topological D-matrix: the numerical study of the $H+H_2$ system

We report here results according to paper **III.** The geometry and the details of the ab-initio calculations are described in section (2.2). Four circular contours are considered for calculating the NACTs; three of them centered at the D_{3h} point and with the radii q=0.3, 0.4, 0.5 Å and the fourth centered at 0.25 Å further away from the HH axis (thus, at a distance of 0.89Å from the HH axis along the symmetry line) with a radius q=0.65Å. In Fig. 3.4 are presented schematically the positions of the various *cis*, the circular contours and the ten φ-dependent NACTs, namely, $\tau_{\varphi jk}(\varphi|q)$; j,k=1,2,3,4,5 as calculated along the various circles. It is important to mention that the points (q,φ=0) and (q,φ=π) are the 'northern' and the 'southern' poles, respectively, both located on the symmetry line. The various figures and mainly a, d, g and j indicate that most of the 'action' takes place around φ = π, the point closest to the HH axis.

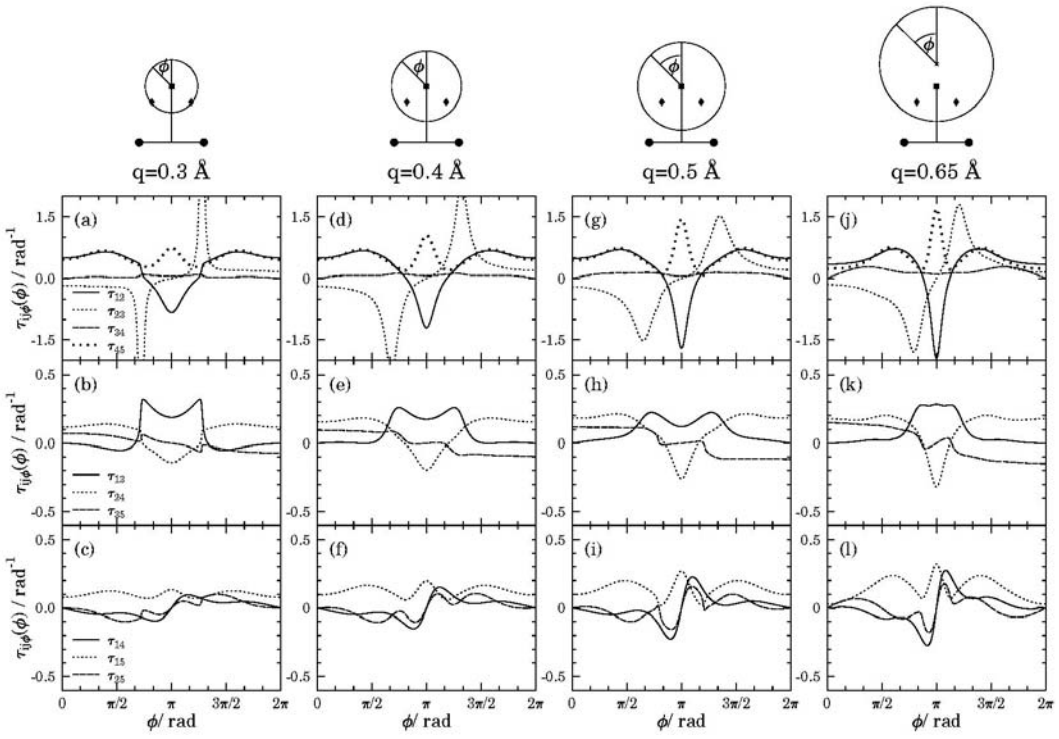

Figure 3.4: Angular non-adiabatic coupling terms, $\tau_{\varphi ij}(\varphi|q)$; i<j, as calculated for the $H+H_2$ system for R_{HH}=0.74 Å

The figures essentially speak for themselves, here we emphasize the large values that are attached to the three adjacent elements $\tau_{\varphi jj+1}$; j=1,2,4, as compared to $\tau_{\varphi 34}$ as well as to all the off-tridiagonal (non-adjacent) elements $\tau_{\varphi jk}$ where k>j+1 (note the different scales of the sub-figures in the two lower rows as compared to the scale of the sub-figures of the upper row). The only exception is $\tau_{\varphi 13}$ which is relatively large. The reason is attributed to the strongly overlapping (1,2) and (2,3) *cis* which are, essentially, the ones to produce the values $\tau_{\varphi 13}$ (see discussion on this subject in Ref. [46]).

Table 3.1 The diagonal elements of the topological **D**-matrix as a function of N, calculated for contours with different radius (q).

N / q /Å	-	3	4	5
0.3	D_{11}	-0.986	-0.810	-0.995
	D_{22}	-0.986	-0.996	-0.996
	D_{33}	+1.000	+0.984	+0.999
	D_{44}	-	-0.798	-0.991
	D_{55}	-	-	-0.990
0.4	D_{11}	-0.966	-0.714	-0.992
	D_{22}	-0.966	-0.993	-0.991
	D_{33}	+0.999	+0.963	+0.997
	D_{44}	-	-0.684	-0.931
	D_{55}	-	-	-0.925
0.5	D_{11}	-0.940	-0.629	-0.986
	D_{22}	-0.938	-0.990	-0.985
	D_{33}	+0.999	+0.936	+0.993
	D_{44}	-	-0.576	-0.931
	D_{55}	-	-	-0.925
0.65	D_{11}	-0.935	-0.614	-0.982
	D_{22}	-0.921	-0.995	-0.982
	D_{33}	+0.986	+0.674	+0.987
	D_{44}	-	-0.293	-0.974
	D_{55}	-	-	-0.961

The various diagonal elements of the **D**-matrix, namely $\mathbf{D}_{jj}(q)$; j=1,..N as calculated for different N-values (i.e. different sizes of Hilbert subspaces) and different circles (expressed in terms of q-values) are presented in Tables 3.1. The results in the table indicate the existence of one (1,2) *ci*, two (2,3) *ci*s and *one* (4,5) *ci* in the configuration space: to demonstrate it, let us choose the diagonals of the **D**-matrix by q=0.3 Å and N=5. Since the contour related to this situation surrounds all the conical intersections (see the geometry which corresponds to the circle q=0.3 Å in Fig. 3.4), applying the formula of Eq. (2.25) we obtain the pattern (-1,-1,+1,-1,-1), namely, only the central wave function does not change sign, which is in agreement with the corresponding $\mathbf{D}_{jj}$ elements.

It is also noticed that adding a fourth state to the three-state Hilbert subspace causes the relevant diagonal **D**-matrix elements to distance themselves from the expected ±1values (Cf. values along the N=3 column and along the N=4 column). The main reason is that in contrast to the three lower states that form a Hilbert subspace the four states do not form a Hilbert subspace and adding the fourth state only increases the background noise (formed by terms like τ_{24} and τ_{14}). However the extension of the four states to five states improves the situation significantly. This is well noticed by inspecting the five diagonal elements of the **D**-matrix as presented in the last column (i.e. N=5). This addition not only improved the four-state **D**-matrix numbers but even the three-state **D**-matrix numbers became much closer to ±1. The above results clearly indicate that adding states of a 'nearby' Hilbert subspace does not necessarily improve the quantization unless one adds a complete nearby Hilbert subspace.

Chapter 4

Field Theoretical Approaches to Calculate Electronic Non-adiabatic Coupling Terms

As it turned out in the previous chapters, the singularity of the NACTs at the position of the conical intersection adds a new dimension in the study of molecular processes. Being singular, hints towards the possibility that the NACTs are a kind of a field that has its origin at these singular points [46,47] which produce non-local effects. The intriguing idea to categorize the singularity points of the NACTs as sources for a field is somewhat reminiscent of the fields produced by charged particles (electrons, protons etc.) and the spatial distribution of the NACTs as the spatial intensity of the field. The aim of this chapter is to show, applying ab-initio calculations, that a theory of this kind is plausible. In section (4.1) a model is represented for a two-state system, which is based on simple vector algebra, while in section (4.2) we apply 'curl-divergency' equations for the three-state system to calculate the NACTs in every desired point of its CS.

4.1. An algebraic-vectorial approach to obtain non-adiabatic coupling field from conical intersections

From now on in this section we concentrate on the two-state systems. The two 'axiomatic' conditions for any molecular system of real Hamiltonian, as we saw in the previous chapter, are the curl condition and the quantization condition. For a two-state Hilbert space these conditions look as follows:

$$curl\boldsymbol{\tau} = 0\,, \tag{4.1}$$

as the expression $[\boldsymbol{\tau} \times \boldsymbol{\tau}]$ in Eq. (2.14) by two-level case vanishes.

$$\oint \boldsymbol{\tau}(R) dR = n\pi \tag{4.2}$$

which is exactly the Equation (2.23) without the index of $\boldsymbol{\tau}$, as here the NACT matrix has only one nonzero element.

However, from Eq. (4.1) and subsequently from Stokes' theorem follows, that the path integral of $\boldsymbol{\tau}$, when $\boldsymbol{\tau}$ is an analytic function, i.e. not enclosing a singularity (namely a *ci*), must vanish. Thus when we encounter a *ci*, at this

particular point of the configuration space, Eq. (4.1) is not valid, we have to modify it on the following way:

$$curl\boldsymbol{\tau} = 2\pi f(\varphi)\frac{\delta(q)}{q}, \tag{4.3}$$

where the position of the *ci* was supposed to be at the origin of the coordinate system, (q,φ) are polar coordinates, δ(q) is the Dirac delta function and f(φ) is some function of the angle φ chosen in such a way to satisfy the condition, given by

$$\int_0^{2\pi} f(\varphi)d\varphi = n\pi\,. \tag{4.4}$$

In what follows f(φ) is defined as the virgin angular component related to a given *ci*. Now Eq. (4.3) with the additional condition in Eq. (4.4) is equivalent with the fulfillment of the curl and quantization conditions in Eq. (4.1-2). In this case after some algebra we obtain that

$$\tau_\varphi(q \sim 0,\varphi) = f(\varphi). \tag{4.5}$$

Since the above pair of Equations (4.1-2) are too general to be solved now we have to apply our model assumption, namely that the virgin radial component, $\boldsymbol{\tau}_q(\varphi,q)$ is always identically zero. Also numerical studies show that $\boldsymbol{\tau}_q(q)$ is finite as $q\to 0$ and is orders of magnitude smaller than $\boldsymbol{\tau}_\varphi(\varphi)/q$ (in this region), therefore we hope that the model will describe quite well the real molecular $\boldsymbol{\tau}$ field. Consequently, when we encounter one single *ci* in the origin of the (q,φ) configuration space, the components of the model $\boldsymbol{\tau}$ field read as follows:

$$\boldsymbol{\tau}_\varphi(q,\varphi) = f(\varphi), \tag{4.6a}$$

$$\boldsymbol{\tau}_q(q,\varphi) = 0\,. \tag{4.6b}$$

Next we consider the situation where the two states form several *ci*s. In this case, just like in case of electric fields, because of the linearity of the curl equation, vector-algebra can be employed to add up the contributions of the various *ci*s to obtain the resultant intensity of the field at an arbitrary given point. Let us attach to each *ci* a different f(φ)-function, i.e. $f_j(\varphi_j)$ to indicate that each such a *ci* may form a different virgin distribution.

The components of the model $\boldsymbol{\tau}$ field are given by the following formulas [46,47]:

$$\boldsymbol{\tau}_q(q,\varphi) = -\sum_{j=1}^{N} f_j(\varphi_j)\frac{1}{q_j}\sin(\varphi-\varphi_j)$$
$$\boldsymbol{\tau}_\varphi(q,\varphi) = q\sum_{j=1}^{N} f_j(\varphi_j)\frac{1}{q_j}\cos(\varphi-\varphi_j) \qquad (4.7)$$

where q and φ are primary coordinates, q_j and φ_j are coordinates related to the position of the j-th *ci*. Eq. (4.7) can be proved to satisfy Eq. (4.1) and Eq. (4.2) provided that the functions $f_j(\varphi_j)$ fulfill the conditions

$$\int_0^{2\pi} f_j(\varphi_j)d\varphi = n_j\pi\,. \qquad (4.8)$$

Thus Eq. (4.7) yields the two components of $\boldsymbol{\tau}(q,\varphi)$, for a distribution of two-state *ci*s expressed in terms of the virgin distributions of the NACTs at their own *ci*s. These functions (i.e. the virgin distributions $f_j(\varphi_j)$) have to be obtained from ab-initio treatments; however the entire field is formed by Eq. (4.7). Next we apply this model for the third and the fourth states of the $Na+H_2$ system. In this case we have four *ci*s and we sum up the contributions of all of them (employing Eq. (4.7)) and compare with ab-inito calculations.

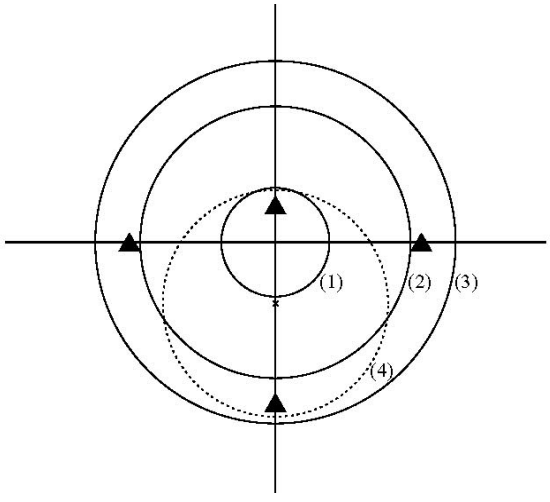

Fig. 4.1. The four (3,4) conical intersections of the $Na+H_2$ system labeled by ▲. The three co-centric circles denoted by (1),(2),(3) with their centers at O(0,0) surrounding different number of conical intersections and the circle (4) with its center at O(0,-0.135a.u.) surrounding the two conical intersections located on the symmetry line.

The main findings for our present purpose are that the third and the fourth states form a quasi two-state Hilbert subspace coupled by the four (3,4) *ci*s. In other words this system furnishes a unique opportunity to apply the vector-algebra for a relatively complicated system with four sources (singularities).

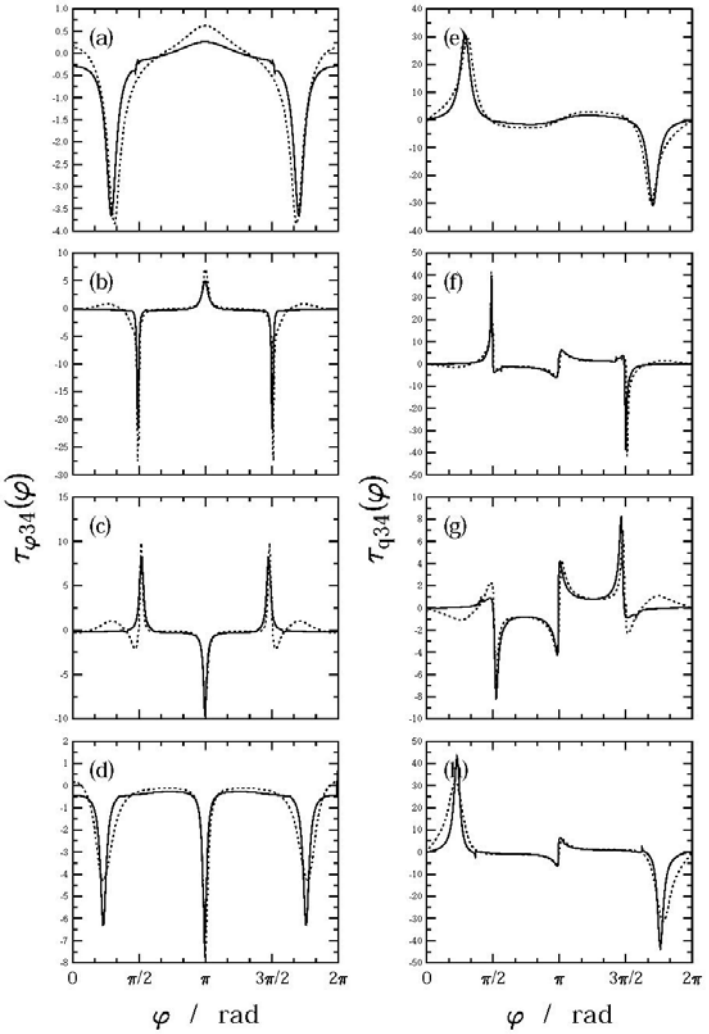

Fig. 4.2. Final results for the $Na+H_2$ system: A comparison between ab-initio and model results for the $\tau_{34}(\varphi|q)$ non-adiabatic coupling term as calculated along four circles presented in Fig. 4.1. In (a), (b), (c) and (d) are presented the angular components, $\tau_{\varphi 34}(\varphi|q)$ and in (e) (f), (g) and (h) are presented the radial components, $\tau_{q23}(\varphi|q)$. Full lines are results due to ab-initio calculations; dashed lines are results due to vector-algebra calculations.

The four *ci*s and the various circles along which the calculations were done are presented in Fig. 4.1. The positions and types of these *ci*s have been described in section (2.2.2). We do not show the virgin distributions here (they can be found in paper **V**), but we note that all of them are of the elliptic type [48] (in contrast to the circular Jahn-Teller type [9]).

The model results and the ab-initio ones are compared in Fig. 4.2. In fact, like in the $H+H_2$ system (can be observed in paper **IV)**, the results speak for themselves. It is noticed that although the ab-initio distributions are frequently quite complicated and show a lot of structure the vector-algebra produces functions that are capable to follow very accurately the ab-initio wiggles.

4.2. A field theoretical approach to obtain non-adiabatic coupling field from conical intersections

The model of the preceding section was based on the assumption that in a given region of interest the Hilbert subspace can be considered with a good approximation two dimensional. However, in several physical situations this assumption does not hold. Increasing the involved region round a two-state conical intersection, the two-level approximation breaks down, and we must take into account more and more states so as the quantization and curl condition are satisfied with a good quality. This feature of the Hilbert subspace can be observed in the model based on the Mathieu equation in section (3.1). Furthermore a conical intersection not the same type, i.e. which couples other states, as the one situated in the origin of the encircled area, can also extend the size of the Hilbert subspace, as we have shown in the analysis of the $H+H_2$ system in section (3.2). That is, we had to consider at least N=3 states to obtain in the diagonal of the **D**-matrix values close to ±1 according to Table 3.1, when we treated a contour involving (1,2) and (2,3) *ci*s as well.

Therefore in the light of the previous remarks, it seems a relevant question how to extend the analysis of section (4.1) to more than two states. In the present section we are dealing with the extension to the case of N=3 state. We derive and solve the molecular 'curl-divergency' equations to obtain the fields produced by the NACTs. In contrast to electrodynamics (and the previous two-state case) we usually encounter more than one field, and moreover the guiding equations are not linear which causes additional complications comparing with the Maxwell equations. The calculations are carried out for the three lower states of the $H+H_2$ system and the results are compared with ab-initio calculations.

Let us start as in the two-state case from first principles, i.e. the equations, which govern the behavior of the fields of NACTs:

One of the set of equations are called the Curl equations. They are coming from the curl condition, defined by Eq. (2.14) and writing in a more explicit form for N=3, we obtain

$$curl\,\tau_{12} = \left[\tau_{23} \times \tau_{13}\right], \tag{4.9a}$$

$$curl\,\tau_{23} = \left[\tau_{23} \times \tau_{12}\right], \tag{4.9b}$$

$$curl\,\tau_{13} = \left[\tau_{12} \times \tau_{23}\right]. \tag{4.9c}$$

The other set of equations is coming from Eq. (2.6). Rearranging and writing separately the equations for each component of $\boldsymbol{\tau}$ we obtain the so-called Divergency equations

$$div\,\tau_{12} = \tau_{12}^{(2)} - \tau_{23}\tau_{13}, \tag{4.10a}$$

$$div\,\tau_{23} = \tau_{23}^{(2)} - \tau_{13}\tau_{12}, \tag{4.10b}$$

$$div\,\tau_{13} = \tau_{13}^{(2)} - \tau_{12}\tau_{23}. \tag{4.10c}$$

where the scalar $\tau_{ij}^{(2)}$ terms according to Chapter 2, are defined by $\tau_{ij}^{(2)} = \left\langle \zeta_i \middle| \nabla^2 \zeta_j \right\rangle$. It is noticed that the Curl-Divergence (C-D) equations (4.9-10) in the case of a two-dimensional parameter space, contain altogether nine unknowns (six due to the two components of $\boldsymbol{\tau}_{12}$, $\boldsymbol{\tau}_{13}$, $\boldsymbol{\tau}_{23}$ and three due to the three scalar $\boldsymbol{\tau}^{(2)}$ terms) which means that the solution is not uniqe unless we introduce some model assumptions, as we did it in section (4.1) by the two-level case. An other complication, that these C-D equations are not linear as can be seen from the rhs. of Eqs. (4.9). Although in paper **VI** we also deal with the problem to find a proper model to the scalar $\boldsymbol{\tau}^{(2)}$ terms, now our aim is not so much to guess this term but rather to form an existence theorem for the molecular fields based on these C-D equations. Therefore, in the further treatment we suppose that the scalar $\boldsymbol{\tau}^{(2)}$ terms are given from some way of approximation, and in the following our purpose is to show that these equations are solvable like in vector-field theory. To clarify the issue, let us see for instance the pair of Equations (4.9a, 4.10a):

$$curl\,\tau_{12} = \left[\tau_{23} \times \tau_{13}\right] = J, \tag{4.11a}$$

$$div\,\tau_{12} = \tau_{12}^{(2)} - \tau_{23}\tau_{13} = \rho. \tag{4.11b}$$

It can be observed that the rhs. of the above equations do not contain $\boldsymbol{\tau}_{12}$, and therefore J and ρ can be considered as the sources of $\boldsymbol{\tau}_{12}$. The statement that a vector-vector function is unambiguously defined by its curl and divergency follows from the theorem of vector calculus, and we demonstrate it below:

Let us form the curl of Eq. (4.11a), then apply the formula $\nabla \times \nabla v = \nabla \nabla v - \Delta v$, we arrive at $\nabla \nabla \tau_{12} - \Delta \tau_{12} = \nabla \times J$, plug in the place of $\nabla \tau_{12}$ from Eq. (4.11b) the source term ρ, and arrange the equation, finally we obtain

$$\Delta \tau_{12} = \nabla \rho - \nabla \times J \tag{4.12}$$

Eq. (4.12) means indeed two scalar Poisson equations (since $\boldsymbol{\tau}_{12}$ is a two-component vector for our planar CS), and the inhomogeneity on the rhs. of Eq. (4.12) is some (not linear) functions of $\boldsymbol{\tau}_{23}$ and $\boldsymbol{\tau}_{13}$. Thus when we suppose that these source terms are given we are able to solve them, and finally as a result obtain $\boldsymbol{\tau}_{12}$. We can obtain the same way from the rest of the pair of Eqs. (4.9-10) $\boldsymbol{\tau}_{23}$ and $\boldsymbol{\tau}_{13}$. Certainly we can pose the question, but where the source term comes from, as in a real situation it is also undetermined. To solve this problem, we put forward an iterative scheme in paper **VI**, starting from a first guess for $\boldsymbol{\tau}_{12}$,$\boldsymbol{\tau}_{23}$ and $\boldsymbol{\tau}_{13}$, then solving Eq. (4.12) for $\boldsymbol{\tau}_{12}$ and the similar equations for $\boldsymbol{\tau}_{23}$ and $\boldsymbol{\tau}_{13}$, then once completed, a new cycle can be started with the modified values. Finally, if the convergency is reached after the *n*the iteration step, we stop, and gain the exact values for the various NACT elements.

Within the numerical study we avoid the task of series of iterations and also the derivation of $\boldsymbol{\tau}^{(2)}$, these issues are out of our present aims. In the numerical study we are more interested in establishing these equations by solving each pair, assuming that the inhomogeneous terms are produced in a straightforward way via ab-initio calculations.

A common way of solving such partial differential equations is to expand the two components of $\boldsymbol{\tau}$, i.e. $\boldsymbol{\tau}_{\varphi}$ and $\boldsymbol{\tau}_{q}$ (working in polar coordinates) in Fourier series with q-dependent coefficients. In the particular calculations we treated approximately 50 terms in the Fourier expansion, which means 2x50 ordinary differential equations (for $\boldsymbol{\tau}_{\varphi}$ and $\boldsymbol{\tau}_{q}$) to be solved with appropriate boundary conditions.

Now we report the numerical details of the calculations for the $H+H_2$ system.

Why do we probe the theory discussed above for the $H+H_2$ system? First of all it is a simple "test" system which is frequently used for various studies connected with electronic non-adiabatic transitions [5,7,17,49]. Secondly, as we showed in section (3.2) by the analysis of this particular system, and mentioned in the beginning of this chapter it yields a Hilbert subspace of three dimensions with a good quality. Mostly it is due to the fact that it lacks (3,4) *ci*s, and therefore the fourth and above states are decoupled from the lower ones, thereby forming the desired three-state Hilbert subspace. The ab-inito study related to produce the NACTs is essentially similar to the one described in subsection (2.2.1).

The Poisson equations are solved for a (circular) region centered at the equilateral D_{3h} *ci* and surrounded by a circle with a radius $q = q_0$ where $q_0 = 0.5$ Å. We mention that exactly this contour is plotted in the geometry of the third column in Figure 3.5.

However, since this region contains the two troublesome (2,3) *ci*s located at about a distance of q~0.29 Å we divided this region into two sub regions: (1) the internal region defined within the (radial) range $0 \le q \le q_i$ where $q_i = 0.285$ Å. (2) the external region defined within the circular strip in the interval: $q_e \le q \le q_0$ where $q_e = 0.295$ Å. Having these two regions the two (2,3) *ci*s are located outside both of them (see Fig. 3.5 to identify the slightly larger contour than q_e in the first column). Now we concentrate merely on the internal region (paper **VI** gives full details about the outer one, and also much more details are found on the inner region).

One Dirichlet-type boundary condition defined along the circle with q_i is derived by ab-initio calculations. At the origin, all five NACTs i.e., $\tau_{\varphi 23}(\varphi,q=0))$, $\tau_{\varphi 13}(\varphi,q=0))$, $\tau_{q12}(\varphi,q=0))$, $\tau_{q23}(\varphi,q=0))$ and $\tau_{q13}(\varphi,q=0))$ are assumed to be identically zero. The only exception is $\tau_{\varphi 12}(\varphi,q=0)$ for which it is assumed to be 0.5 $Rad.^{-1}$, as was verified on numerous occasions (Ref.[7,50] or see paper **III**). In Figs. (4.3) and (4.4) are presented the angular and the radial components of τ_{12}, τ_{23}, respectively, as calculated along various circles surrounding the D_{3h} *ci*. As it is noticed the fit is essentially very promising for the two components of the three τ-matrix elements (the missing τ_{13} is shown in paper **VI** and can be checked there).

The ability of the Poisson equations to produce such encouraging fits has to be appreciated because of two reasons: (1) the initial integration point is the D_{3h} *ci* point, namely, a singular point. (2) boundary conditions were attached only

to one boundary (and not two as is usually the case) and therefore play a relative minor role in these calculations.

Fig 4.3 **Fig 4.4**

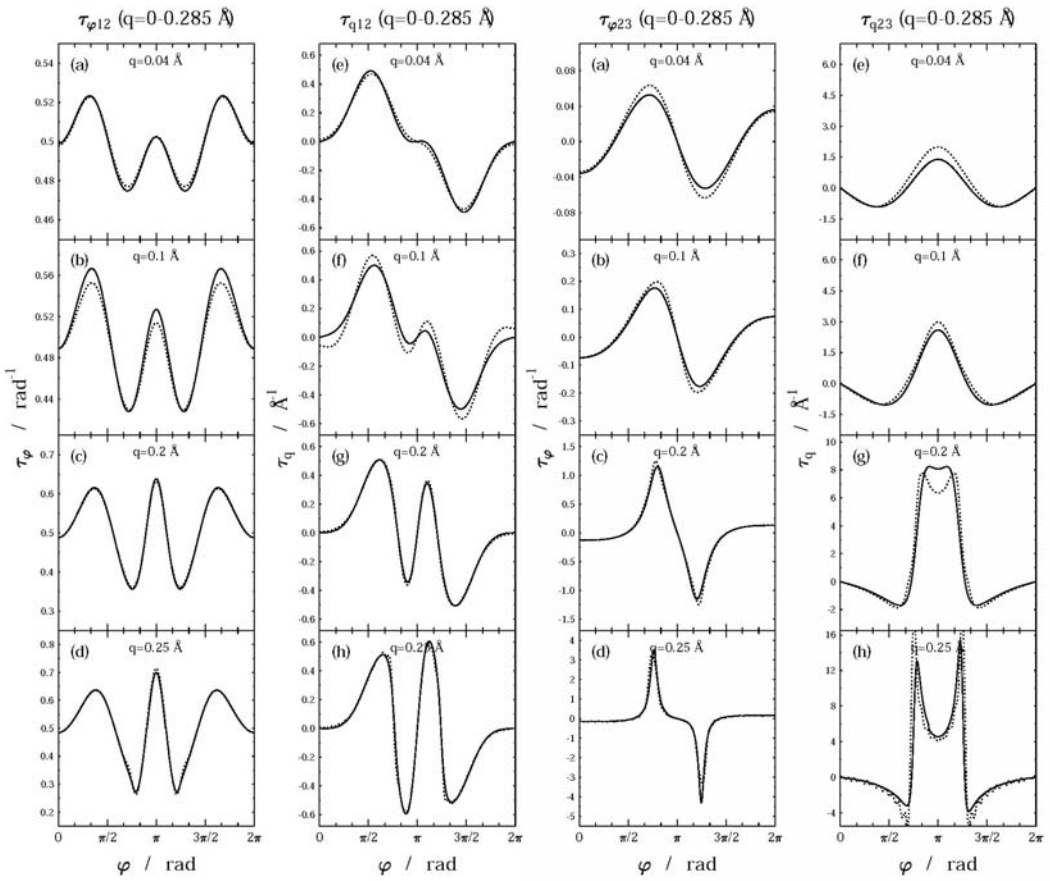

Fig. 4.3&4.4 Results for the (1,2) and (2,3) NACT $\boldsymbol{\tau}$, i.e. $\boldsymbol{\tau}_{\varphi 12}$,$\boldsymbol{\tau}_{q12}$ and $\boldsymbol{\tau}_{\varphi 23}$,$\boldsymbol{\tau}_{q23}$ as calculated along the specified co-centric circles centered at the equilateral (1,2) D_{3h} *ci* are presented as a function of φ, the angular coordinate. All specified circles are in the internal region. Full line: results are due to ab-initio calculations; dotted line results are due to the Poisson equations solved for the ab-initio inhomogeneities. In the sub-figures (a) – (d) are presented results for the angular component $\boldsymbol{\tau}_{\varphi 12}$ and sub-figures (e)-(h) are present results for the radial component $\boldsymbol{\tau}_{q12}$. The Dirichlet (ab-initio) boundary conditions are given along the circle with the radius q=0.285 Å.

Chapter 5

Topological Effects in the Diabatic Framework

In this chapter we investigate molecular systems via the diabatic picture, which can be given by Eq. (2.11):

$$\mathbf{W} = \mathbf{A}^{\mathrm{T}}\mathbf{u}\mathbf{A} \tag{5.1}$$

We show in section (5.1) that in the diabatic framework we can reveal the distribution of degeneracies with the aid of various methods. We also derive that a well defined sign can be attached to each conical intersection. In section (5.2), the theoretical outcomes are illustrated via numerical examples for the $Na+H_2$ system and we also explain some mysterious features of the so-called twin *ci*s with the aid of this theorem. This chapter is mainly based on the results of the papers **VII** and **VIII**. It is noted that from now on we are interested in the two-dimensional Hilbert space for the sake of simplicity.

5.1. The theory

The diabatic Hamiltonian for the two-level case in Eq. (2.10b) can be further written as

$$\hat{H}_{dia} = \hat{T}_N + \mathbf{W} = \left(\hat{T}_N + \Sigma\right)\mathbb{1} + \begin{pmatrix} v(R) & u(R) \\ u(R) & -v(R) \end{pmatrix}, \tag{5.2}$$

where $\Sigma(R) = (u_1 + u_2)/2$ is the average of the lower (u_1) and upper (u_2) potential energy surfaces. Thus the new diabatic potential **W** decoupled from a scalar term $\sum$ looks as follows:

$$W = \begin{pmatrix} v & u \\ u & -v \end{pmatrix}, \tag{5.3}$$

where the functions *v*, and *u* are identified as the diabatic potential surfaces. We saw in Chapter 2 that the solution of the differential equation $\nabla\mathbf{A} + \boldsymbol{\tau}\mathbf{A} = \mathbf{0}$ can be expressed by Eq. (2.19). The solution in the two-level case simplifies to the following expression:

$$\mathbf{A}(R) = \begin{pmatrix} \cos(\gamma(R)) & \sin(\gamma(R)) \\ -\sin(\gamma(R)) & \cos(\gamma(R)) \end{pmatrix}, \tag{5.4}$$

where the γ mixing angle is given in terms of the following line integral [24]:

$$\gamma(R_f) = \gamma(R_{\mathbf{s}}) + \int_{Rs}^{R_f} \tau(R) dR \,. \tag{5.5}$$

Let us denote the γ mixing angle with α when the contour is closed and eliminate the index from the NACT as we did it in sec. (4.1) (as in the two-state case the NACT matrix has only one nonzero element). Now substituting the expression (5.3) to the definition of the diabatic potential **W** in Eq. (5.1) we obtain the functions *v* and *u* expressed by the angle γ and the difference of the adiabatic energy surfaces:

$$\begin{aligned} u &= \frac{1}{2}(u_2 - u_1)\sin(2\gamma), \\ v &= \frac{1}{2}(u_2 - u_1)\cos(2\gamma). \end{aligned} \tag{5.6}$$

After some manipulation of the above set of equations (see in paper **VIII**), we obtain

$$\exp(2i\gamma) = \frac{u + iv}{\sqrt{u^2 + v^2}} = f(u,v) \,. \tag{5.7}$$

The preceding equation indicates an explicit connection between the angle γ and the *u,v* elements of the matrix **W**: let the R nuclear coordinates be varied round a closed loop. Because of the quantization condition expressed by Eq. (2.23), and choosing in Eq. (5.5) the arbitrary $\gamma(R_s)$ to be equal to zero, we obtain for the angle γ after the full cycle

$$\alpha = n\pi. \tag{5.8}$$

This means regarding to Eq. (5.7) that the function on the rhs. of Eq. (5.7) describes a number of n circles on the (*u,iv*) complex plane. Let us label the points on the contour Γ where *u*(R)=0 as 'z-points', and where *v*(R)=0 as 'p-points'. Thus when traversing the contour Γ, we encounter a series of z- and p-points. The main outcome of the Eq. (5.7) that when we inspect merely the sequence of z- and p-points we can follow the function $f(u,v)$ on the unit circle of the complex (*u,iv*) plane. Thus after traversing the loop Γ, finally we obtain the number of n circles, and the equality $\alpha = n\pi$ in Eq. (5.8) yields the final mixing angle α.

Now let us approach the same problem from an other point of view. According to the curl condition in Eq. (2.14) when **τ** is an analytic function of the coordinates R,

$$curl\,\tau = 0 \,. \tag{5.9}$$

As we noted in section (4.1) the only points in the two-dimensional configuration space R, where $\boldsymbol{\tau}$ could be a discontinuous function, are the positions of the degeneracies. Thus applying Stokes' theorem by excluding the area of the vicinity of degeneracies we arrive at the following formula for the mixing angle:

$$\alpha = \oint_{\Gamma} \tau dR = \sum_{i=1}^{k} \oint_{ci} \tau dR \,, \tag{5.10}$$

where the number of degeneracies are denoted by *k*, and the contour integral of the rhs. of Eq. (5.10) is performed round each point of degeneracy. Next we suppose that each degeneracy in the area of interest is formed by a conical intersection. Now let us concentrate on one single *ci* assuming at the point of (x=0,y=0), where x,y denotes Cartesian coordinates. Expanding **W** in a Taylor expansion about the degenerate point we find $\mathbf{W} = \mathbf{W}^{(n)} + \mathbf{W}^{(n+1)} + \ldots$, where $\mathbf{W}^{(n)}$ collects all elements of order n in the nuclear displacements. For conical intersections the **W** diabatic potential varies linearly in the function of the nuclear coordinates near the position of the *ci* and only the leading n=1 term will survive:

$$\begin{aligned} u &= c_{11}x + c_{12}y \\ v &= c_{21}x + c_{22}y \end{aligned}, \tag{5.11}$$

where the c_{ij} linear-coefficients can be represented with the elements of a $2x2$ matrix **C**.

Eq. (5.11) represents an affine transformation $C : \Re^2(x,y) \to \Re^2(u,v)$, while Eq. (5.7) represents a continuous, nonlinear function F from the $S = (u,v)$ plane to the circle S^1. Thus $F \circ C$ maps the circle S^1 in (x,y) to the circle S^1 in (u,v).

In paper **VIII** we prove that the $F \circ C$ transformation maps the counterclockwise moving circular path $S^1(x,y)$ to a circular path $S^1(u,v)$ with the same orientation when $\det \mathbf{C} > 0$, and reverses the orientation when $\det \mathbf{C} < 0$.

Now considering the above result we conclude, that circling round a conical intersection with an infinitesimal radius we obtain n=±1, and γ for the closed loop according to Eq. (5.8) can take up altogether two values $\alpha = \pm\pi$ depending on the sign of det **C**. This result means that there exist two groups of *ci*s which we call negative and positive ones, depending on the sign of the corresponding α. Let us denote the number of negative *ci*s inside the loop Γ with K and the

number of positive *ci*s with L, then we can write further Equation (5.10) and obtain

$$\alpha = \oint_{\Gamma} \tau dR = (L - K)\pi \,. \tag{5.12}$$

Next we summarize the two main results of the present section:

(1) For a system of 2x2 real **W** diabatic potential, the mixing angle α for a closed contour Γ in the two-dimensional configuration space can be calculated by inspecting the sequence of z and p points (i.e. the zeros of the *u,v* diabatic potentials).

(2) α for the same closed contour is determined by the difference of the number of positive and negative *ci*s.

Thus the connection between the above observations yields practical methods to determine the distribution of conical intersections inside the loop merely by inspecting the zeroes of the elements of the diabatic potential **W**.

5.2. Concrete numerical methods

In subsection (5.2.1) we give two methods on the basis of the results of section (5.1) to yield different kinds of information regarding the existence of *ci*s in a given region. Then in subsection (5.2.2) we give an explanation of the observed α mixing angle for twin *ci*s in the C_2H molecule applying again the theory of section (5.1).

5.2.1 Numerical study of the Na+H_2 system

To be more specific we consider the $3^2A'$ and the $4^2A'$ states of the Na+H_2 system, as it was found in paper **I** that in the near region of the group of (3,4) *ci*s (see Fig. 2.1.b) the states $3^2A'$ and $4^2A'$ form to a good approximation a Hilbert subspace and therefore can be diabatized (almost) rigorously. In Fig 5.1 are presented the locations of the (3,4) *ci*s and three circular contours where the elements *u,v* of the diabatic potentials will be formed.

Now we give a brief description (a more detailed account can be seen in paper **VII**) about the concrete procedure we obtain the α mixing angles for the various circles in Fig. 5.1. First of all, the ab-initio calculation yields the u_1 and u_2 adiabatic potential surfaces and the NACT elements, which in this special two-level case means only one element of $\boldsymbol{\tau}$. Then choosing a base point we

calculate the γ mixing angle according to Eq. (5.5) and substituting to Eq. (5.6) the ab-initio u_1,u_2 and γ, we obtain the function *u* and *v*.

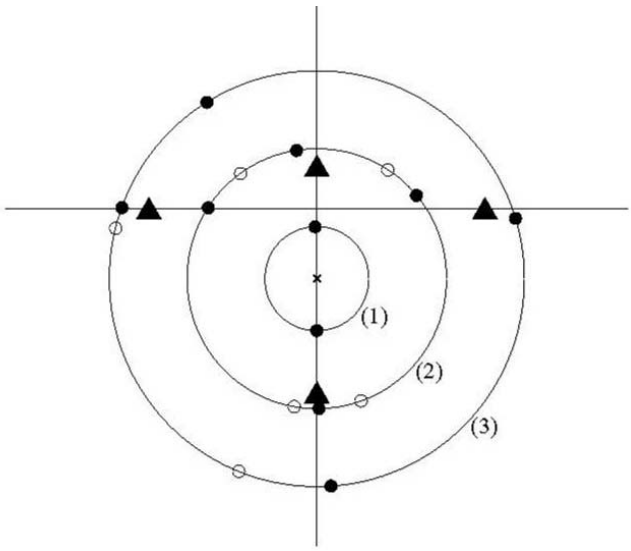

Fig. 5.1 The four ab-initio (3,4) conical intersections of the $Na+H_2$ system and the three co-centric circles with radii q=0.1, 0.25, and 0.4 a.u., surrounding different number of conical intersections. The empty (○) and the full circles (●) are the positions of the intersection points between the circles and the equi-u=0 and the equi-v=0 lines respectively. These points form along each circle the sequence of 'zp' points discussed in this chapter.

Fig. 5.2 shows these functions on the three co-centric circles drawn in Fig. 5.1 in the function of the angular coordinate φ (where φ=0 rad denotes the upper intersection point of the symmetry axis and the circular contour). As it is noticed for the circle with the smallest radius q=0.1 a.u. only the *v*(q,φ) crosses (twice) the abscissa and as a result the (p,p) series is formed thus indicating that no *ci* is surrounded by this circle, as indeed is the case (see Fig. 5.1). For q=0.25 a.u. we obtain a more complex pattern, namely we have a (p,z,p,z,p,z,p,z) sequence which means that the function *f* in Eq. (5.7) makes two circles (i.e. n=2) and according to Eq. (5.8) results in α=2π. It indicates by inspecting the positions of *ci*s in Fig. 5.1 that this particular circle with q=0.25 a.u. surrounds two *ci*s of the same kind, and moreover they are both positive *ci*s. The pattern of 'zp' sequence for q=0.4 a.u. is (p,p,z,z,p,p), which means that no circle was traced out by the function *f* in Eq. (5.7), thus yielding the

value α=0. This result indicates that the other two *cis* situated symmetrically on the both sides of the symmetry line must be also of the same kind, but in this case they are both negative *cis*.

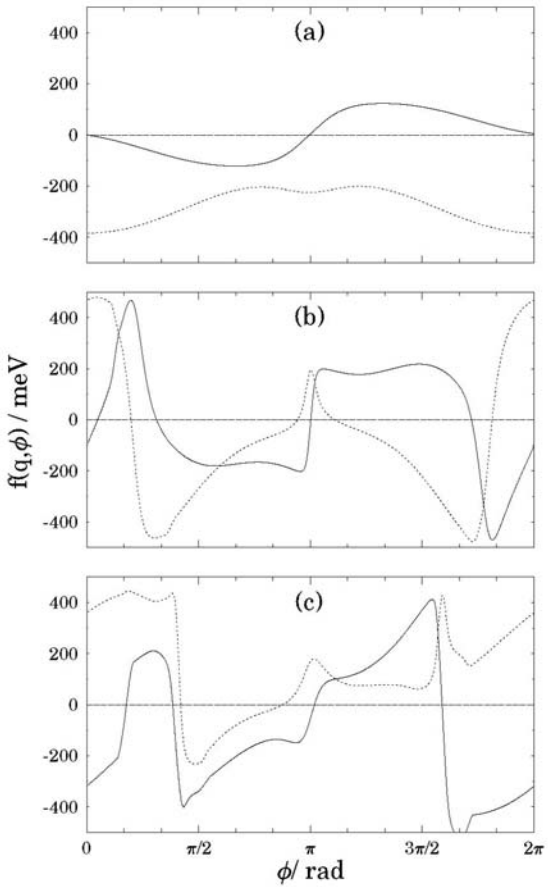

Fig. 5.2 The diabatic potentials f(q,φ)=u(q,φ) (dashed lines) and f(q,φ)=v(q,φ) (full lines) as calculated along the various circles in Fig 5.1: (a) Results along a circle with q= 0.1 a.u.; (b) Results along a circle with q= 0.25 a.u.; (c) Results along a circle with q= 0.4 a.u.

In the following we show an other method, which reveals not only the difference of the negative and positive *cis* inside the given contour, but can detect the exact positions of *cis* as well. Let us choose now the origin of several co-centric circles as the intersection of the two perpendicular axis (as it can be seen in Fig. 5.3) but with different radii to cover the whole region of interest. Calculating the same way as in Fig. 5.1 for each circle the 'zp' points and

connecting the neighboring ones with each other, we obtain the contours along which either $v(q,\varphi)=0$ (full lines) or $u(q,\varphi)=0$ (dashed lines).

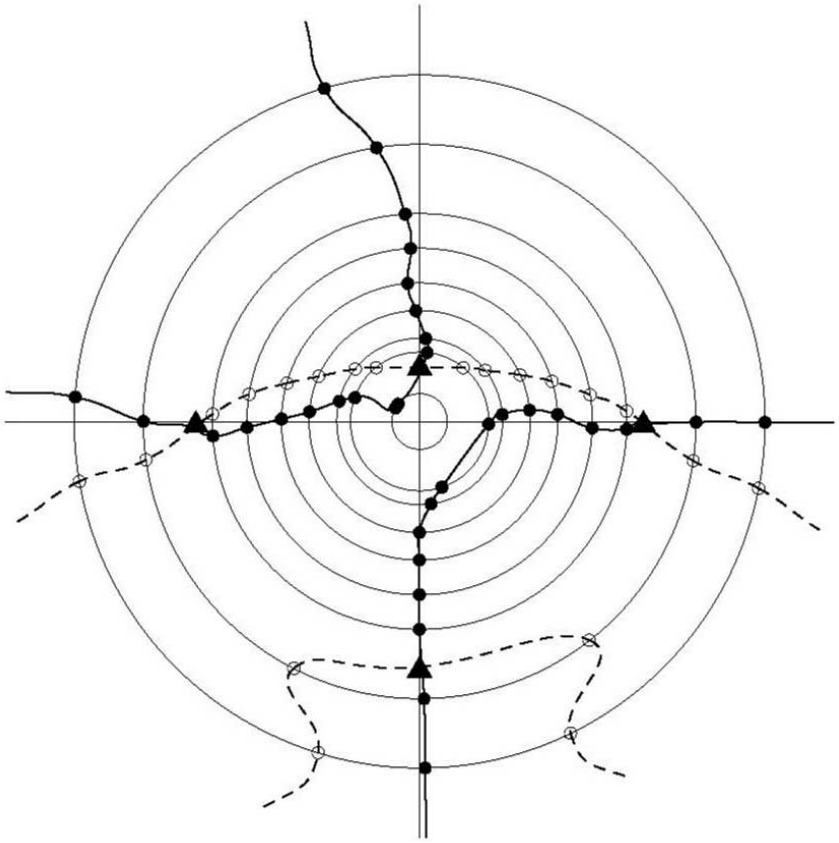

Fig. 5.3 The equi-u=0 (dashed lines) and the equi-v=0 (full lines) as calculated for the 3-rd and the 4-rth adiabatic states of the $Na+H_2$ system. The points (empty circles,○ and full circles, •) are the 'zp' points along the various circular contours. It is noticed that all the intersections between the equi-u=0 lines and the equi-v=0 lines are at the points of the *ci*s (▲).

Upon inspecting Fig. 5.3 we can notice two interesting features of the figure: The dashed curves (equi-u=0) and full curves (equi-v=0) cross each other only at the point of degeneracies, and on the other hand always one full line and one dashed line intersect at these points.

We are able to explain and support these two observations based on the results of sec. (5.1). First let us see Eq. (5.6). According to it, whenever $u_1=u_2$ (i.e. we encounter degeneracy) it zeroes both the function u and v. Conversely, the occurrence of $u=0$ and $v=0$ at the same point of the configuration space can

happen only when $u_1=u_2$ (since cos2γ and sin2γ can never take up the same value for any γ). This means that indeed the two types of curves can intersect only at a point of degeneracy. Now taking into account Eq. (5.11) in the closed vicinity of a conical degeneracy the functions *u* and *v* are linear functions of the coordinates, therefore it implies just one equi-u=0 line and one equi-v=0, which cross each other. In this way we established that the degeneracies, we encounter in Fig. 5.3 are really conical (opposite to the parabolic one [51]).

In summary, investigating the diabatic framework we concluded to a rather elaborated procedure, which not only yields the exact positions of all *ci*s in a region of interest, but also we could decide whether the particular degeneracy is conical (and can produce topological effect) or just a parabolic one (which is actually a Renner-Teller type [52,53], and not causing topological effect).

5.2.2 Application for the annihilation of twin *ci*s

In Section 5.1 we obtained that there exist two groups of *ci*s, depending on the sign of α, called as positive or negative *ci*s. However, conical intersections are in general not exist as isolated points but as continuous seams of dimension N^{int}-2 (N^{int} is the number of internal coordinates) for the nonrelativistic Coulomb Hamiltonian. A tri-atomic system is characterized by three internal coordinates, which implies that the surface of intersection in this particular case has a dimension 1, and is referred to it as a seam (so far we encountered only the dimension 0, i.e. points of intersections, but it was due to freeze one internal coordinate).

In paper **VIII** we proved that the sign attached to the point of *ci* can be generalized to attach to the seam of *ci* as well, i.e. the seam has also a definite sign (plus or minus) on a segment which is not crossed by other seam. This can be symbolized by an arrow aligned parallel to the seam on the following way: let us define an ε unit vector parallel to the seam in the sense of the right-hand screw rule, then if the type of the seam is plus, it should point in the same direction as ε, otherwise it would point in the opposite direction.

In the following applying the above results about the definite type of seams we describe the phenomenon of pair-annihilation of twin *ci*s.

Twin *ci*s were found in AlH_2 between the potential energy surface of $^2B_2$ and $^2A_1$ within C_{2v} symmetry [54] and also in C_2H molecule between the two lowest $1^2A'$ and $2^2A'$ electronic states and between the $3^2A'$ and $4^2A'$ states [42,55]. These later *ci* twins are located at relatively small distance on the two sides of the C_{2v} line. Here it was further found that the separation between the

twins could be made arbitrary small by varying the CC relative positions, and even they can be brought into coincidence at some CC position, i.e. they annihilate each other.

When calculating the line integral of τ on the contour Γ_{12} which surrounds both *ci*s (see in Fig. 5.4 plane A), it was found that the circulation was identically zero [55]. If we suppose that the area bounded by Γ_{12} is very small (indeed we can make it arbitrary small by tuning the CC distance just before to the coalescence), then τ vector-field fulfills the two-state 'curl-condition', i.e. Eq. (4.1), and we can write

$$\oint_{\Gamma_1} \tau dR + \oint_{\Gamma_2} \tau dR = \oint_{\Gamma_{12}} \tau dR = 0. \tag{5.13}$$

The second equality was due to the observation, thus according to the definition of α mixing angle $\alpha(\Gamma_1) = -\alpha(\Gamma_2)$. Namely, it was obtained that in the present case the signs attached to the twin *ci*s are opposite [55]. In Ref. [55] the question was arisen if it is a general or an accidental feature of *ci*s, to arrange themselves in such a way to be of opposite signs. It was stated there, also due to other observations, that it looks to be typical for all merging *ci*s.

Now, considering that the sign of seam is definite (either plus or minus), we can give a clear explanation for it, which on the other hand support and confirm the statement of [55]. Fig. 5.4 shows the process how two conical intersections merge and annihilate each other, which in the three-dimensional configuration space can be described as two approaching seams with opposite signs (signed by the arrows pointing to opposite directions) meat at the point P. However, an other but likewise legitimate description is that we consider it as **only one seam**, which gently touch the plane B in the point P (causing a Renner-Teller type crossing [53]) and then turn back. Notice that this description also suits the opposite sign-directions of *ci* seams: seeing that, when we follow the curve of seam, locally the direction of the arrow must not flip, but globally it will change direction. Thus the arrow attached to the seam pierces the plane A twice, once it points up and once down, which correspond to opposite signs, hence yielding for the circulation of τ round the circuit Γ_{12} zero.

In conclusion we established that the pair-annihilation of *ci*s can be considered as a process which is formed by one seam, hence by construction this guarantees the opposite signs of the coalescing conical intersections.

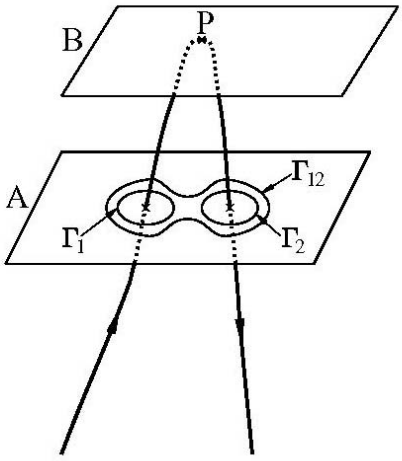

Fig. 5.4 A segment of the infinite long seam of conical intersection, and two intersecting planes (A,B). On the plane A, it is drawn contours (Γ_1, Γ_2) encircling their own *ci*s, and a contour (Γ_{12}) encircling both of them. The seam touches the plane B in the point P and then turns back. The sign of the seam is denoted by arrows, once pointing up and after the 'turning point P' pointing down. Each Γ contour is oriented counterclockwise.

Chapter 6

The Geometric Open-Path Phase Revisited: Application to Born-Oppenheimer Molecular Systems

While dealing with the interference of light, Pancharatnam came up with a brilliant idea regarding a general phase of the evolution for a polarized light [32], which was then generalized to an arbitrary quantum evolution [33]. In this chapter we analyze semi-classically the evolution of nuclei in molecular systems thereby gaining insight in the notion of the Pancharatnam phase factor (termed as open-path phase) and establishing various connections with the mixing angle as well. The theoretical findings will be supported by numerical study carried out for the ($Na+H_2$) molecular system.

6.1. Theoretical considerations

When a system evolves from an initial state $|\psi(0)\rangle$ to a final state $|\psi(t)\rangle = \hat{U}(t)|\psi(0)\rangle$ with a unitary evolution operator $\hat{U}(t)$, we refer to γ_t as the phase of $|\psi(t)\rangle$ relative to $|\psi(0)\rangle$ once we have

$$\langle\psi(t)|\psi(0)\rangle = e^{i\gamma_t}\left|\langle\psi(t)|\psi(0)\rangle\right|. \tag{6.1}$$

For an arbitrary quantum evolution, the geometric Pancharatnam phase can be defined as [Samuel] $\gamma_p = \gamma_t - \gamma_d$, where

$$\gamma_d = -(1/\hbar)\int_0^t \langle\psi(t)|\hat{H}|\psi(t)\rangle dt \tag{6.2}$$

is the dynamical phase, with the Hamiltonian of the system $\hat{H}$. Let us denote with ρ the magnitude of the overlap $\langle\phi(t)|\phi(0)\rangle$, where $|\phi(t)\rangle$ differs from $|\psi(t)\rangle$ that its dynamical phase factor, defined by Eq. (6.2) has been removed.

Next, our aim is to gain the γ_p geometric phase and the magnitude ρ according to their definitions above (coming from the dynamical treatment of the system), and then we try to find connection with the γ mixing angle (coming from the time-independent treatment of the molecular system).

From now on we restrict our attention only on two-level systems, since the numerical example at section (6.2) will be based on the analysis of $Na+H_2$, a two-state system in the region of our interest. The general treatment and the corresponding three-state numerical example for $H+H_2$ can be also found in paper **IX**. We note that the generalization is straightforward, and below the two-state case will also show the relevant results of this survey.

Consider the quantum system whose normalized state vector $|\psi(t)\rangle$ evolves according to the Schrödinger equation

$$i\hbar\frac{d|\psi(t)\rangle}{dt} = \hat{H}_{el}|\psi(t)\rangle\,, \tag{6.3}$$

where $\hat{H}_{el}$ stands for the electronic Hamiltonian which parametrically depends on the nuclear coordinates (i.e. we apply the semi-classical treatment of the composite system). Next assuming that the Hilbert subspace is two-dimensional in a given region Λ in the configuration space, we can write

$$\psi(t) = \tilde{\zeta}_1(R(t))|\zeta_1(R_0)\rangle + \tilde{\zeta}_2(R(t))|\zeta_2(R_0)\rangle\,, \tag{6.4}$$

where $\tilde{\zeta}_1(R(t))$ and $\tilde{\zeta}_2(R(t))$ are coefficients which depend solely on the nuclear coordinates and $\{|\zeta_i(R_0)\rangle\}_{i=1}^2$ are the electronic eigenfunctions of the electronic Hamiltonian $\hat{H}_{el}$ according to Eq. (2.3) in a given fixed point R_0 in Λ. The substitution of Eq. (6.4) into Eq. (6.3) yields the equation to be solved:

$$i\hbar\frac{d\tilde{\zeta}(R(t))}{dt} = \mathbf{W}(R(t))\tilde{\zeta}(R(t)), \tag{6.5}$$

where $\tilde{\zeta}(R(t))$ is a column vector formed by $\tilde{\zeta}_1(R(t))$ and $\tilde{\zeta}_2(R(t))$, $\mathbf{W}$(R) is the 2x2 diabatic potential matrix related to the two eigenstates of the two-level system. Above we utilized the fact that besides the definition of Eq. (2.11) $\mathbf{W} = \mathbf{A}^{\mathbf{T}}\mathbf{u}\mathbf{A}$ there exists an other one defined in paper **X**, originating from the diabatic representation of the nuclear Schrödinger equation, namely [38]

$$\mathbf{W}_{jk} = \langle\zeta_j(R_0)|\hat{H}_{el}(R)|\zeta_k(R_0)\rangle\,. \tag{6.6}$$

Now we recall Eq. (2.11) defining **W**(R) and Eq. (5.4) defining the 2x2 ADT matrix, **A**(R):

$$\mathbf{A}(R)=\begin{pmatrix}\cos(\gamma(R)) & \sin(\gamma(R))\\ -\sin(\gamma(R)) & \cos(\gamma(R))\end{pmatrix},$$

where γ(R) is the mixing angle, discussed in section (5.1) and defined by Eq. (5.5). Then further we suppose circular contours in Λ, thus we can switch from R→(q,φ(t)), then multiplying Eq. (6.5) by **A**(R), and carrying out a few other algebraic changes yield the following two coupled equations to be solved:

$$\begin{aligned}\frac{d\eta_1}{dt}&=-\frac{i}{\hbar}u_1\eta_1+\tau_\varphi\frac{2\pi}{T}\eta_2\\ \frac{d\eta_2}{dt}&=-\frac{i}{\hbar}u_2\eta_2-\tau_\varphi\frac{2\pi}{T}\eta_1\end{aligned}, \tag{6.7}$$

where τ_φ is the angular component of the NACT, and $\eta(t)=\begin{pmatrix}\eta_1(t)\\ \eta_2(t)\end{pmatrix}$ is given as $\eta(t)=A(t)\tilde{\zeta}(t)$. Here we supposed that the velocity of the nuclei is constant along the contour, and takes a finite T time to complete the cycle (i.e. the time period is T). To solve Eq. (6.7) we need initial conditions for η: for this purpose we assume at t=0 the **A**-matrix is diagonal (i.e. γ(R(t=0))=0 and R_0=R(t=0)) and the lower state is the initial state, so that the initial conditions for $\tilde{\zeta}(t)$ are: $\tilde{\zeta}(t=0)=\begin{pmatrix}1\\0\end{pmatrix}$ and consequently $\eta(t=0)=\begin{pmatrix}1\\0\end{pmatrix}$. It is noticed that in Eq. (6.7) the coupling term is inversely proportional to T, consequently once T→∞ (the adiabatic limit) the coupling vanishes, and as a result $\eta_2\to 0$ which implies that $\tilde{\zeta}_1(t)$ takes the form:

$$\lim_{T\to\infty}\tilde{\zeta}_1(t)\to\exp\left(-\frac{i}{\hbar}\int_0^t u_1(t)dt\right)\cos\gamma\,. \tag{6.8}$$

Now let us recall the definition of the open-path (Pancharatnam) phase discussed in the beginning of this section, and let us calculate $\langle\psi(t)|\psi(0)\rangle$. With the above defined initial conditions, $\psi(t=0)=|\zeta_1(R_0)\rangle$ and thus $\langle\psi(t)|\psi(0)\rangle=\tilde{\zeta}_1(t)$. Thus according to Eq. (6.1) we gain γ_t as the argument of $\tilde{\zeta}_1(t)$, i.e. γ_t reads

$$\gamma_t = \arg(\cos(\gamma)) - \frac{1}{\hbar}\int_0^t u_1(t)dt \qquad (6.9)$$

Because of the definition $\gamma_p = \gamma_t - \gamma_d$, and noticing that in Eq. (6.2) the dynamical phase γ_d becomes in the adiabatic ($T\to\infty$) limit $\gamma_d = -(1/\hbar)\int_0^t u_1(t)dt$, we obtain for the open-path phase in the adiabatic evolution the following expression:

$$\gamma_p = \arg(\cos(\gamma(t))). \qquad (6.10a)$$

On the other hand the definition of ρ (in the beginning of this section) leads in the adiabatic limit to

$$\rho = |\cos(\gamma(t))|. \qquad (6.10b)$$

The Eq. (6.10a) means that the open-path phase becomes a step-function so that every time the $\cos(\gamma(t))$ flips its sign, namely, when $\gamma(t) = (2n+1)\pi/2$, the open-path phase γ_p jumps by an odd number of π's.

6.2. Applications

Eqs. (6.10a-b) constitute the main result of the preceding section, namely in case of the adiabatic limit, the ADT angle γ(φ) (formed by BO eigenfunctions) determines unambiguously both the magnitude ρ of the electronic time-dependent eigenfunction (after the removal of the dynamical phase) and its open-path phase γ_p.

In order to understand the meaning of these results we describe first a general molecular system for which this approach is applicable and then analyze numerical results for a specific case.

We assume a (molecular) system of electrons and nuclei which is composed of two, relatively rigid parts but these two parts are 'floppy', the one with regard to the other. Next, at time t=0 an external electromagnetic field is turned on that causes the two parts to revolve, the one with respect to the other. Assuming the molecular system to be in a given BO eigenstate this rotational motion may induce transitions to other states with (oscillating) time dependent probabilities. In the numerical section a time dependent semi-classical treatment is carried out to calculate these probabilities as well as the open-path phase.

The specific system chosen for this purpose is the $Na+H_2$. In particular we concentrated on the $3^2A'$ and $4^2A'$ states which as we could see in subsections (2.2.2) and (5.2.1) of this work are affluent with *ci*s (altogether four) and that these two states are only weakly coupled to the other states of the system and therefore form, approximately, an isolated Hilbert subspace of two dimensions. The ab-initio magnitudes required for the present numerical study to solve Eq. (6.7) are the electronic eigenvalues of the two relevant $3^2A'$ and $4^2A'$ states (u_1,u_2) and the corresponding τ_φ (the angular component of the NACT) along the contours, the two floppy parts of the molecule (in this case Na and H_2) may trace due to the external field. To calculate the open-path phase γ_p we first solve numerically the coupled differential equations in Eq. (6.7) with the aid of the Mathematica package, then obtain $\eta(t)$ and via the relation $\tilde{\zeta}(t) = A^T(t)\eta(t)$ we obtain $\tilde{\zeta}(t)$ as well. Since the components of $\tilde{\zeta}(t)$ determine the time-dependent wave function $\psi(t)$through Eq. (6.4), we can use the same procedure as in Eq. (6.1)-(6.2) to gain both the open-path phase γ_p and after the removal of the dynamical phase factor from $\psi(t)$, the amplitude ρ.

The results are presented in Fig. 6.1 which is divided into three columns and each column is further divided into three sub-figures. The upper sub-figure contains the geometry, namely, the four (3,4) *ci*s (labeled as ▲) and the corresponding circular contours assumed to be created by an external field. In the sub-figure below are presented the amplitudes $\rho(t)$ as derived, once for a finite T-value – to be designated T_{fi} – namely, a value that does not yield adiabatic limit and, once for a large T-value – to be designated T_{ad} – namely, a value that does yield the adiabatic limit. In addition are presented the absolute values of the cosine function, namely, $|\cos(\gamma(\varphi(t))|$ (see Eq. (6.10b)). In the third sub-figure are presented the open-path phases, $\gamma_p(t)$, as calculated, once for $T=T_{fi}$ (the non-adiabatic case) and once for $T=T_{ad}$ (the adiabatic case) as well as the mixing angle γ. We add a few comments related to the presented results:

(1) In all three cases (i.e. on the three different contours in Figs. 6.1(a), (c) and (e)) the amplitude $\rho(t)$, in the non-adiabatic limit (by time period T_{fi}), is quite oscillatory and does not reveal any features of particular interest. However, the amplitude $\rho(t)$, in the adiabatic limit (by time period T_{ad}) is smooth and for all practical purposes is identical to $|\cos(\gamma(t))|$ as, indeed, is indicated by the theory (see Eq. (6.10b)).

(2) It is well noticed that in all three cases, the open-path phase $\gamma_p(t)$ in the non-adiabatic limit ($T=T_{fi}$), forms continuous functions, oscillating to some extent whereas in the adiabatic limit ($T=T_{ad}$) one forms Heaviside-type step

function (see Figs. 6.1(b), (d), (f)). It is obvious that these open-path phases do not show any particular relation with the corresponding mixing angles γ (which are also shown in the respective sub-figures (b), (d) and (f)). However, the theory tells us to look for the cosine of these functions and, indeed, a connection exists in case of the adiabatic case ($T=T_{ad}$): the discontinuous steps for the open-path phases $\gamma_p(t)$ happen exactly at t-values for which cos (γ(t)) changes sign or the γ(t) angles are odd multiples of (π/2).

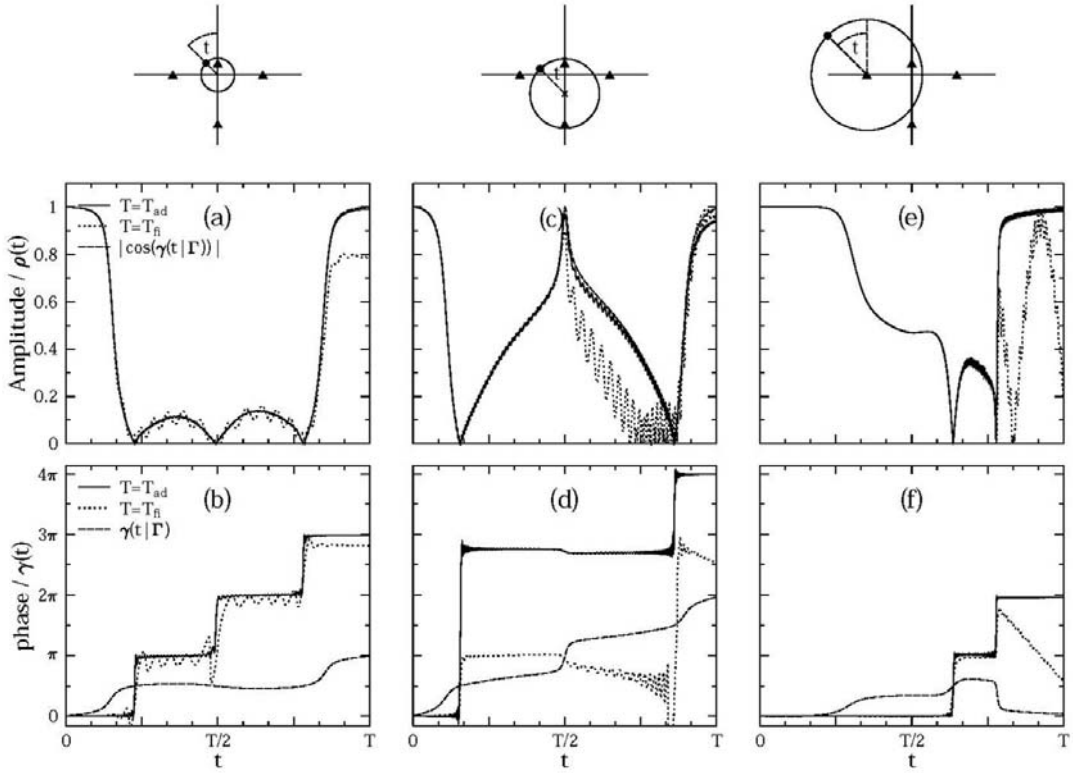

Fig. 6.1 Results for the ab-initio Na+H_2 system as calculated along three circles surrounding different number of (3,4) conical intersections (labeled as ▲). In subfigures (a), (c), and (e) are presented the amplitudes ρ(t) as calculated for $T=T_{fi}$ and $T=T_{ad}$, and the absolute value of the corresponding ADT matrix element $A_{11}(\varphi(t)|\Gamma)$ $=|\cos(\gamma(\varphi(t)|\Gamma))|$. In sub-figures (b), (d), and (f) are presented $\gamma_p(t)$, as calculated once for $T=T_{fi}$ and once for $T=T_{ad}$. The periods $T_{ad} = 2\times10^4, 3.2\times10^4, 8\times10^4$ and $T_{fi} = 3\times10^3, 2.9\times10^3, 1.5\times10^4$ a.u, respectively. It is noticed that the curves for ρ(t) as calculated for $T=T_{ad}$ and the corresponding |cos(γ(t))|-function as obtained from the ab-initio treatment are overlapping so strongly that they are hardly distinguishable.

In summary, in this study we showed theoretically (supported by numerical calculations) that the mixing angle γ formed by BO eigenfunctions determines uniquely both the time-dependent magnitude $\rho(t)$ and the open-path phase $\gamma_p(t)$ of the electronic functions in the adiabatic limit.

Chapter 7

Summary of the Results

The work presented in this thesis deals with many facets of the role of conical intersections in non-adiabatic effects and the role of producing non-local topological effects. In the previous four chapters (Chapter 3-6) four different aspects of the effect of conical intersections in molecular systems were concerned:

(I) in which extent the *ci* determines the dimension of the isolated Hilbert subspace in a given region of the nuclear configuration space, which encircles various number of *ci*s

(II) whether it is possible to claim that the NACTs can be considered as fields which have their sources at the points of conical intersections

(III) whether it is possible, that the Longuet-Higgins' sign change theorem had a generalization for two-level systems, which could be applied in the diabatic framework to reveal the distribution of conical intersections in the configuration space of the molecular systems

(IV) whether there is a relationship in a semi-classical treatment of the molecular systems between the elements of the ADT matrix and the open-path phase of the electronic wave functions in an adiabatic evolution.

The main purpose of this work was to study the tasks posed above. In the following I summarize the main achievements of my work related to this thesis, and thereby give an answer for the above (I)-(IV) questions:

(I)

- I implemented a program for calculation of the **F**-matrix based on Eq. (2.13) and the **D**-matrix based on Eq. (2.16), suitable for any dimension.
- A numerical study is carried out applying the eigenfunctions of the Mathieu equation to study the **D**- and **F**-dependence on the size of configuration space parametrized by x and the number of eigenstates N.

- An ab-initio study is carried out on the $H+H_2$ system by calculating the topological **D**-matrix for N=2…5 states and for various circles with radii 0.3 Å $\leq x \leq$ 0.65 Å.
- Given the **D-** and **F**-matrix I examined the fulfillment of the quantization and curl conditions for given (x,N) values
- I draw the conclusion: a given group of states forms with a good approximation an isolated Hilbert subspace in a given region, when each state, coupled by conical intersections is involved in the group. However, the addition of other states (which are not coupled by *ci*s) to the group further improves the isolation of Hilbert subspace from the rest of the states. The extent of the isolation was measured both by the quantization of the **D**-matrix, and the curl of the **F**-matrix.

(II)

- Based on a model assumption, that the *ci* produces a zero radial component of NACT I implemented a program to calculate the NACT, when the Hilbert subspace is formed by two states. The program employs vector-algebra to add up the contributions of the various *ci*s to obtain the resultant intensity of the field of NACT at an arbitrary given point.
- The comparison between the ab-inito results of the $Na+H_2$ system as obtained from the MOLPRO and the analytical results follow from my program undoubtedly indicates that, indeed, the field of NACT is created by sources located at the degeneracy points formed by the Born-Oppenheimer adiabatic states.
- It is shown that the Curl-Divergence equations (Eq. (2.14) and Eq. (2.16)) as formed within a given N=3-state Hilbert subspace can be converted into a set of inhomogeneous coupled Poisson equations.
- I solved these Poisson equations for a given set of circular boundary conditions employing Fourier series for the three lower states of the $H+H_2$ system and the results are compared with ab-initio calculations for which a very encouraging fit is found like in the two-state case.

(III)

- I derived that the mixing angle of the two-dimensional ADT matrix round a two-state conical intersection can take up the values $\pm\pi$, (termed the related *ci* as positive or negative depending on the sign) which supports the ab-initio results as well.

- I found an explicit use of this fact, describing the phenomenon of pair annihilation of twin *ci*s.
- Here I showed a method to exhaust all topological information from the elements of the two-state diabatic potentials on a given contour in the configuration space. This method yields the difference of the amount of positive and negative *ci*s inside the contour, which I illustrated via numerical examples for the $Na+H_2$ system.
- A procedure, based on results of the preceding paragraph has been developed (and implemented for the $Na+H_2$ system), which is more elaborate than the other method above and requires more numerical efforts, but yields the exact positions of all the *ci*s in the region of interest.

(IV)

- I analyzed molecular systems via the semi-classical framework. My main theoretical finding is that the mixing angle γ of the ADT matrix formed by BO eigenfunctions determines uniquely the γ_p open-path phase of the electronic functions in the adiabatic limit of the evolution.
- The theory predicts that the open-path phase in the adiabatic limit becomes a step-function so that every time the $\cos(\gamma(t))$ (i.e. the diagonal element of the 2x2 ADT matrix) flips its sign, the open-path phase γ_p jumps by an odd number of π's.
- I carried out a numerical study for the ($Na+H_2$) system by exhausting from the time-dependent wave functions the open-path phase both in adiabatic and in non-adiabatic evolutions. The numerical results fit very well the theoretical predictions in the adiabatic case, and also yield useful information about the non-adiabatic case.

Az értekezés összefoglalása

A molekuladinamikai folyamatok kvantummechanikai leírására a fizika és kémia egyik leggyakrabban használt közelítési módszere az 1927-ben kidolgozott Born-Oppenheimer-féle (BO) adiabatikus közelítés, amely az elektronok és a jóval nehezebb atommagok mozgásának szétválasztásán alapul. Az adiabatikus közelítésben a dinamikai jellemzők számítása két részből tevődik össze: az elektron hullámfüggvények és energiák rögzített atommagoknál történő számításából (amely a modern kvantumkémia fő feladata), valamint a magmozgás jellemzőinek számításából az előzőleg meghatározott potenciális energia felületek (PES) segítségével. Bár a BO-közelítés gyakran elegendő pontosságú a molekuláris sajátságok és folyamatok kívánt szintű megértéséhez, a jelenségek egy csoportja (amely ezen értekezés tárgyát is képezi) nem írható le egyetlen potenciálfelület figyelembevételével. A BO- közelítés olyan atomi konfiguráció esetén érvényes, amikor az elektron energiák jól elkülönülnek egymástól. Olyan konfiguráció esetén, amikor a két állapot energiája megegyezik, vagyis az állapotok elfajultakká válnak, a közelítés nem alkalmazható. Ilyenkor átmenetek jönnek létre az egyes adiabatikus elektronállapotok között, melyekért az úgynevezett nem-adiabatikus csatolási tagok (NACT) felelősek. Abban az esetben, ha a fenti jelenség egzakt leírását szeretnénk megkapni, a BO-közelítés helyett annak Born-Huang- kiterjesztését kell használnunk.

Nagyon sok olyan kémiai folyamat létezik a természetben (ide tartozik a legtöbb fotokémiai reakció is), amikor egy molekuláris rendszerben degenerált állapotok lépnek fel, és ezáltal indokolttá válik a Born-Huang-egyenletek alkalmazása. Ezért fontos feladat ezen degeneranciák helyeinek meghatározása. Longuet-Higgins 1975-ben kifejlesztett egy olyan topológiai eljárást, amellyel úgynevezett kúpszerű metszéspont (*ci*) típusú degeneranciák helyei térképezhetők fel. Azt a meglepő eredményt találta, hogy amikor a többatomos rendszer egy zárt hurkot ír le az atommagok konfigurációs terében, olyan módon, hogy a kontúr körülvesz egy *ci* típusú degeneranciát, a degeneranciához tartozó elektron hullámfüggvényeknek előjelet kell váltaniuk. Amikor majd egy évtizeddel később Berry bevezette a geometriai fázis fogalmát, vált világossá, hogy Longuet-Higgins teszt módszere éppen egy, valós függvényekre teljesülő alesete a geometriai fázisnak. Nem sokkal Berry felfedezését követően a róla elnevezett Berry fázis, amely eredetileg a kvantumrendszer ciklikus és adiabatikus időfejlődésére vonatkozott, még általánosabb esetekre is kiterjesztésre került.

Mead és Truhlar mutatott rá először 1980-ban, hogy Longuet-Higgins felfedezése a hullámfüggvény előjelváltására vonatkozólag nem csak a *ci*-k felkutatására alkalmazható, hanem erős hatással lehet az atommagok dinamikájára is. Az elektron hullámfüggény előjelváltásának kompenzálására egy vektorpotenciál taggal egészítették ki a nukleon Schrödinger-egyenletet (SE), ezáltal biztosítva a teljes hullámfüggvény egyértékűségét. Mivel így az egyenlet formailag (és topológiai következményeit tekintve is) teljes analógiát mutat az Aharonov-Bohm féle vektorpotenciált tartalmazó Schrödinger-egyenlettel, a jelenség a „molekuláris Aharonov-Bohm effektus" (MAB) elnevezést kapta. Kupperman és csoportja volt az első, aki ezen MAB effektust konkrét kémiai reakcióban is tetten érte. A MAB effektust is figyelembe vevő elméletileg számolt hatáskeresztmetszetük bizonyos energiákon nagyon szép egyezést mutatott a kísérleti eredményekkel. Ugyanakkor meg kell jegyeznünk, hogy az ezen MAB hatást is tartalmazó nukleon SE, lényegében egy egy-állapot Schrödinger-egyenlet, ezért természetesen az egyes elektronállopotok közötti átmeneteket nem írhatja le jól. Talán ez lehet az oka annak is, hogy az összhang a számított és kísérleti értékek között csak bizonyos energiákon mutatkozott. Nagy energiájú kémiai folyamatok egzakt leírásához a nukleon Schrödinger-egyenletnek szükségszerűen több (gerjesztett) állapotot is tartalmaznia kell, amelyet, mint említettük, a Born-Huang-kép adhat.

Összefoglalva azt állapíthatjuk meg a fenn elmondottakból, hogy a *ci*-k kémiai folyamatokban betöltött hatását alapvetően két különálló részre bonthatjuk. Egyfelől a MAB hatás révén határfeltételt szabnak ki az atommag hullámfüggvényére, vagyis a konfigurációs térben egy nemtriviális topológiát idéznek elő, másfelől a szomszédos elektronállapotok csatolása révén lehetővé teszik, hogy a rendszer egyszerre több elektronállapotban is létezhessen. A Born-Huang-kép, mivel közelítést nem tartalmaz, elviekben jól kell, hogy leírja mindkét hatást. Ezen dolgozat fő témája, annak vizsgálata, hogy az elvileg precíz Born-Huang-leírás milyen kényszerek és korlátozások árán válik alkalmazhatóvá a molekuláris rendszerek dinamikai vizsgálatában.

Az adiabatikus Born-Huang-kép két ab-initio mennyiségen alapszik: a potenciális energia felületeken és a nem-adiabatikus csatolási tagokon. Ezen fenti két mennyiség egzakt ismerete elvileg teljes mértékben meghatározza a molekuladinamikát. Azonban rögtön egy nagyon súlyos gyakorlati probléma merül fel, amikor a Born-Huang-egyenleteket egy degeneranciákkal is rendelkező rendszerre szeretnénk megoldani. A NACT-nak ugyanis a degeneranciák helyén pólusa van, amely a Born-Huang differenciál-egyenletek

megoldásában numerikus problémákat, instabilitásokat okoz. Egy elméleti módszer ezen probléma kiküszöbölésére az adiabatikus Born-Huang-képből a diabatikus képbe történő áttérés egy unitér-transzformáció (ADT mátrix) segítségével. Ezáltal a szingularitásokkal rendelkező NACT-okat kitranszformáljuk, és helyette a diabatikus képben egy potenciálcsatolást nyerünk, ami már analitikus függvénye lesz a koordinátáknak. Az ezen transzformáció véghezviteléhez szükséges ADT mátrix egy adott kontúron történő előállításához Baer 1975-ben javasolt egy módszert több-atomos molekulák esetére, egyben feltételt adva arra nézve is, hogy mikor létezhet pontos megoldás. Ezen ún. 'rotációs feltétel' a NACT-okból képezhető **F**-mátrixra nulla értéket ír elő az adott kontúr minden egyes pontjában. Nevezzük a zárt kontúrhoz tartozó ADT mátrixot **D**-mátrixnak. Nemrégiben Baer megmutatta, hogy ha az ADT mátrix megoldása az egész kontúr mentén létezik, akkor ez a **D**-mátrixra egy kvantálási feltételt szab ki. Az is megmutatható, hogy mind a rotációs, és mind a kvantálási feltételek teljesülnek, ha az elektron sajátfüggvények egy teljes Hilbert teret feszítenek ki a konfigurációs tér azon részében, ahol az ADT mátrix megoldását keressük. Az **F**=0 feltétel differenciális (csak a konfigurációs tér adott pontjára vonatkozó), míg a **D** kvantáltsága integrális (az egész kontúr mentén teljesítendő) feltétel a teljes Hilbert tér eldöntésére vonatkozólag.

Ezen értekezés négy fő fejezetének megfelelően (3-6. fejezetek) négy különböző szemszögből tárgyalom a *ci*-k szerepét a nem-adiabatikus és topológiai effektusok létrehozásában. A következőkben pontokba szedve ismertetem ezen témákat és a hozzá fűződő eredményeimet:

(I) Mint ahogy fentebb már említettük, az ADT mátrix kulcsfontosságú szerepet játszik a diabatikus képbe való áttérés során. A helyes kvantummechanikai leírás pedig, ha a rendszer elfajult állapotokkal rendelkezik, csak a diabatikus képben történhet. Emiatt bármilyen információ az ADT mátrixról fontos lehet a nem-adiabatikus folyamatok precíz leírásához. Amennyiben az elektronállapotok teljes Hilbert teret alkotnak, az ADT mátrix egzaktul előállítható, és így a nyert diabatikus kép is egzakt. Sajnos azonban a többatomos molekulák tipikusan olyan kvantumrendszerek, amelyek végtelen bázisban élnek, ami végtelen dimenziós ADT mátrix-hoz vezet és ilyen formában a problémát kezelhetetlenné teszi. Arra keressük a választ, hogy lehetséges-e a teljes Hilbert teret mégis jó közelítéssel kis, N=2…5 dimenziós alterekre bontani, úgy, hogy egy adott alteren belül az állapotok közötti csatolás erős legyen, de a különböző alterek között csak gyenge csatolódás lépjen fel. Ez

esetben az egyes állapotok csoportjai egymástól elszigetelődnének, ami azt jelenthetné, hogy numerikusan elegendő lenne az ezen állapotokhoz tartozó Hilbert altereket egymástól függetlenül kezelni, amely a probléma komplexitását lényegesen lecsökkentené. A feladatom tehát, különböző rendszerek numerikus vizsgálata volt, a fent megfogalmazott kérdésre keresve a választ:

- Egy programot készítettem, amely alkalmas tetszőleges N dimenziós **F**- és **D**-mátrixok kiszámítására az adott rendszer NACT elemeinek ismeretében.
- A Mathieu-egyenlet sajátfüggvényein alapuló modellre vizsgáltam, hogyan függenek az **F**- és **D**-mátrixok a konfigurációs tér nagyságát mérő x paramétertől, és az állapotok N számától.
- Ab-initio számítást végeztem a $H+H_2$ rendszer NACT elemeinek meghatározására a MOLPRO program segítségével, amelyből a **D**-mátrixot állítottam elő különböző N=2…5 állapotszámok és 0.3 Å $\leq x \leq$0.65 Å sugarú körvonalak mentén.
- A fenti **F**- és **D**-mátrixok ismeretében vizsgáltam mind a modell, mind a valós molekuláris rendszerre a kvantálási és a rotációs feltételek teljesülésének mértékét.
- Az eredményekből a következőket állapítottam meg: Tegyük fel, hogy a minket érdeklő atomi konfigurációs térben, kiválasztunk egy Hilbert alteret. Ezen alteret alkotó állapotok a fenti konfigurációs térben akkor fognak a teljes Hilbert tér többi állapotától elszigetelt Hilbert alteret alkotni, ha minden olyan állapot szerepel a fenti altérben, amely a minket érdeklő tartományban elfajulttá válik. Ugyanakkor, ha ezen Hilbert altérhez további olyan állapotokat adunk, melyek nem csatolódnak *ci*-n keresztül az eredeti Hilbert alteret alkotó állapotokhoz, tovább növekszik az így keletkezett Hilbert altér izoláltsága a „külvilágtól". Az izoláltság mértékét a **D**-, és **F**-mátrixok adják meg.

(II) Sikerült kimutatnom, hogy az ADT mátrix dimenziószáma lényegesen redukálható és egyértelmű kapcsolatban áll a *ci* típusú degeneranciáknak a konfigurációs térbeni elhelyezkedésével, viszont még további időigényes ab-initio számításokat igénylő feladat a NACT mátrix elemeinek előállítása. Ezért az volt a szándékunk, hogy a NACT-okat lehetőleg egyszerű modelleken alapuló módszerrel, az ab-initio számításokat megkerülve kaphassuk meg jó közelítéssel. A modellfeltevés: a *ci*-k, mint pólussal rendelkező szingularitások generálják a NACT vektorteret, az elektrodinamika egyenleteinek forrásaihoz

hasonló módon. Míg N=2 esetén az analógia szépen nyomon követhető, és egy vektor-algebrai modellhez vezet, addig N=3 esetén csatolt, nemlineáris téregyenletekhez jutunk a nem-Abeli vektortérnek megfelelően:

- Abból a modellfeltevésből kiindulva, hogy a *ci* által generált NACT mező radiális komponense zérus, egy programot készítettem, amely a két-dimenziós konfigurációs tér bármely pontjában kiszámítja az N=2 esetén előálló NACT komponensét.
- Összehasonlítva az $Na+H_2$ rendszer ab-initio és a fenti model NACT komponenseit, megállapíthatjuk, hogy a *ci,* mint a NACT vektorteret keltő forrás jól modellezi a valós esetet N=2 állapot esetén.
- Megmutattam, hogy a NACT-ok egyes komponensei közötti kapcsolatot leíró ún. rotáció-divergencia egyenletek N=3 állapot esetén három csatolt Poisson-egyenletre vezetnek.
- Ezen Poisson-egyenleteket Fourier-sorfejtésen alapuló numerikus módszerrel oldottam meg a $H+ H_2$ rendszer három legalsó állapotára, figyelembe véve az adott ab-initio határfeltételeket. Az így kapott NACT elemek az ab-initio eredményekkel szép egyezést mutatnak, hasonlóan az N=2 állapot esetéhez.

(III) Amikor a rendszerben egy viszonylag nagy méretű konfigurációs térben előforduló degeneranciák azonos állapotokat csatolnak össze, a kapcsolódó elszeparált Hilbert altér az előző tanulmányaink alapján jó közelítéssel N=2 dimenziósnak adódik. Ezt a tényt felhasználva, hasznosnak találtuk, hogy behatóbban tanulmányozzuk két-állapot rendszerek diabatikus potenciálját abból a célból, hogy mélyebb ismereteket nyerhessünk a *ci*-k eloszlására vonatkozóan. Ezúton konkrét kapcsolatot találtunk egy adott kontúr diabatikus potenciáljának viselkedése, és a kontúrt határoló konfigurációs térben található *ci*-k száma és elhelyezkedése között. Ez a módszer a Longuet-Higgins-féle topológiai teszt általánosításának tekinthető a diabatikus reprezentációban. Konkrét eredményeim a következők:

- Levezettem, hogy a *ci* körülvétele során adódó kétdimenziós ADT-mátrix ún. forgási szöge $\pm\pi$ értékeket vehet fel. A *ci*-t a π előjelétől függően pozitívnak, vagy negatívnak nevezzük. A $\pm\pi$ érték helyességét konkrét valós molekuláris rendszerekből származó ab-initio eredmények is alátámasztják.
- Felhasználva a fenti eredményt, magyarázatot adtam a „*ci* párok megsemmisítését” leíró jelenségre.

- Megmutattam, hogy a 2x2-es diabatikus potenciálnak egy adott kontúron felvett értékeiből következtetni lehet a kontúron belül található *ci*-k előjeles összegére. Ezen eredményt az $Na+H_2$ rendszerre numerikusan is igazoltam.
- Egy eljárást fejlesztettem ki (és ugyancsak alkalmaztam az $Na+H_2$ rendszerre), amely az előző pont eredményeire épít, bár lényegesen több ab-initio, és numerikus számítást igényel annál, de képes a rendszer degeneranciáinak egzakt meghatározására.

(IV) Mindezidáig az időtől független Born-Huang-kép eszköztárát vizsgáltuk: a NACT, az ADT vagy a diabatikus mátrixokat, abból a célból, hogy a nem-adiabatikus folyamatok dinamikájának megoldására (illetve megoldhatóságára) vonatkozólag hasznos információkat szolgáltassanak. Most a molekuláris rendszereket egy másik, ún. félklasszikus szinten vizsgáljuk: feltételezzük, hogy a molekulának egyik atommagját egy külső elektromágneses potenciállal mozgatjuk, melynek hatására az így módon két részre tagolódó rendszer egymáshoz képest forgó, keringő mozgást végezhet. Ha a rendszert egy kezdeti (mondjuk alapállapotból) indítottuk el, akkor ezen fenti mozgás hatására gerjesztett állapotokba történő átmenetek jönnek létre. Ha a fenti mozgatás viszonylag lassú (ún. adiabatikus) nagy keringési idővel, akkor ez pontosan egy olyan szituáció, ahol értelmezhető a Berry fázis: az a fázisfaktor, amelyre egy állapot tesz szert azáltal, hogy nagyon lassú mozgással a rendszer paraméterterében egy zárt körutat tesz meg. 1988-ban Samuel és Bhandari megmutatta, hogy Berry geometriai fázisa általánosítható a kvantumrendszer tetszőleges nem ciklikus és nem adiabatikus időfejlődésére is. Mind a Berry, és mind pedig az általánosított ún. nyílt görbe menti geometriai fázist vizsgáltam molekulák szemiklasszikus közelítésében, és a következő eredményekre jutottam:

- Az ADT mátrix γ forgási szöge teljes mértékben meghatározza a nagyon lassú, adiabatikus időfejlődésű molekuláris rendszer γ_p nyílt görbe-menti geometriai fázisát.
- Az elmélet szerint, a nyílt görbe-menti fázis adiabatikus időfejlődés során ugrás-függvényt vesz fel, ahol az ugráshelyek a $\cos(\gamma(t))$ függvény, azaz a 2x2-es ADT mátrix diagonális elemének zérushelyei, és az ugrások nagysága π páratlan számú többszörösei.
- Az elmélethez kacsolódó numerikus számításokat az ($Na+H_2$) rendszeren végeztem, kinyerve a rendszer időfüggő hullámfüggvényéből a nyílt görbe-menti geometriai fázist mind nagyon

lassú adiabatikus, mind pedig nem-adiabatikus időfejlődés során. A numerikus eredmények az adiabatikus esetben szinte teljes átfedésben vannak az elméleti jóslatokkal, és ugyancsak hasznos információt szolgáltatnak a nem-adiabatikus időfejlődésre nézve.

Acknowledgements

I would like to express my deepest gratitude to my supervisor Ágnes Vibók for her constant support and guidance during these years.
I am also greatly indebted to Michael Baer for introducing me to the field of non-adiabatic coupling terms, and for numerous interesting discussions.
I would also like to acknowledge Gábor Halász for his scientific help in numerical computations.
Finally, I thank the members of the Department of Theoretical Physics at the University of Debrecen for their steady help and encouragement.

Bibliography

[1] M. Born and J.R. Oppenheimer, Ann. Phys. (Leipzig) 84, 457 (1927).
[2] M. Born and K.Huang, Dynamical Theory of Crystal Lattices, Oxford University Press, Oxford, UK, 1954, pp. 166-177 and 402-407.
[3] G. Herzberg and H.C. Longuet-Higgins, Discuss. Faraday Soc. 35, 77 (1963).
[4] D.G. Truhlar and C.A. Mead, Phys. Rev. A68, 032501 (2003).
[5] S.L. Mielke, B.C. Garett, and K.A. Peterson, J. Chem. Phys. 116, 4142 (2002).
[6] S. Han, D.R. Yarkony, J. Chem. Phys. 119, 5058 (2003).
[7] G.J. Halász, Á. Vibók, A.M. Mebel, M. Baer, J. Chem. Phys. 118, 3052 (2003).
[8] D.R. Yarkony, J. Phys. Chem. A 101, 4263 (1997).
[9] H. A. Jahn and E. Teller, Proc. Roy. Soc. (London) A161, 220 (1937).
[10] H.C. Longuet-Higgins, Proc. R. Soc. London A344, 147 (1975).
[11] H. C. Longuet-Higgins, Adv. Spectrosc. 2, 429 (1961).
[12] C.A. Mead and D.G. Truhlar, J. Chem. Phys, 70, 2284 (1979).
[13] C.A. Mead, Chem. Phys. 49, 23 (1980).
[14] M. V. Berry, Proc. Roy. Soc. London, A392, 45 (1984).
[15] Y. Aharonov and D. Bohm, Phys. Rev. 115, 485 (1959).
[16] C.A. Mead, Chem. Phys. 49, 33 (1980).
[17] Y.M. Wu, B.Lepetit, and A. Kuppermann, Chem. Phys. Lett. 186, 319 (1991).
[18] D.A.V Kliner, D.E. Adelman, and R.N. Zare, J. Chem. Phys. 95, 1648 (1991).
[19] Z.H. Top and M. Baer, J. Chem. Phys. 66, 1363 (1977).
[20] R.K. Preston and J.C. Tully, J. Chem. Phys. 54, 4297 (1971).
[21] W. Lichten, Phys. Rev. 164, 131 (1967).
[22] Z.H. Top and M. Baer, Chem. Phys. 25, 1 (1977).
[23] W.D. Hobey, A.D. Mclachlan, J. Chem. Phys. 33, 1695 (1960).
[24] M. Baer, Chem. Phys. Lett. 35, 112 (1975).
[25] M. Baer, A. Alijah, Chem. Phys. Lett. 319, 489 (2000).
[26] H.J. Werner and P.Knowles, MOLPRO, Version 96.3, University of Birmingham, U.K., 1996.
[27] H. Dachsel, R. Shepard, J. Nieplocha, and R. Harrison, J. Com. Chem. 18, 430 (1997).

[28] H. Lischka, M. Dallos, P.G. Szalay, D.R. Yarkony, and R. Shepard, J. Chem. Phys. 120, 7322 (2004).
[29] D. Suter, K.T. Mueller, and A. Pines, Phys. Rev. Lett. 60, 1218 (1987).
[30] T. Bitter and D. Dubbers, Phys. Rev. Lett. 59, 251 (1987).
[31] P.G.Kwiat and R.Y. Chiao, Phys. Rev. Lett. 66, 588 (1991).
[32] S. Pancharatnam, Proc. Indian Acad. Sci. A 44, 247 (1956).
[33] J. Samuel and R. Bhandari, Phys. Rev. Lett. 60, 2339 (1988).
[34] M. Baer, Chem. Phys. 259, 123 (2000).
[35] H. Hellmann, Einfuhrung in die Quantenchemie, Franz Deutiche, Leipzig, 1937.
[36] R.P. Feynman, Phys. Rev. 56, 340. (1939).
[37] G.A. Worth and M.A. Robb, Adv. Chem. Phys. 124, 355 (2002).
[38] M. Baer, Mol. Phys. 40, 1011 (1980).
[39] M. Baer, Phys. Rep. 358, 75 (2002).
[40] H.J. Werner and W. Meyer, J. Chem. Phys. 74, 5794 (1981).
[41] B. Lengsfield and D.R. Yarkony, Adv. Chem. Phys. 82 (part 2), 1 (1992).
[42] C.A. Mead, J. Chem. Phys. 78, 807 (1983).
[43] A.M. Mebel, M. Baer, S.H. Lin, J. Chem. Phys. 112, 10703 (2000).
[44] M. Baer, R. Englman, Mol. Phys. 75, 283 (1992).
[45] R. Englman, A. Yahalom, M. Baer, Int. J. Quantum Chem. 90, 266 (2002).
[46] M. Baer, A.M. Mebel, and G.D. Billing, Int. J. Quantum Chem., 90, 1577 (2002).
[47] J. Avery, M. Baer, and G.D. Billing, Molec. Phys. 100, 1011 (2002).
[48] M. Baer, A.M. Mebel and R. Englman, Chem. Phys. Lett. 354, 243 (2002).
[49] R. Abrol and A. Kuppermann, J. Chem. Phys. 116, 1035 (2002).
[50] G.J. Halasz, A. Vibok, A.M. Mebel and M. Baer, Chem. Phys. Lett. 358, 163 (2002).
[51] J.W. Zwanziger, E.R. Grant, J. Chem. Phys. 87, 2954 (1987).
[52] R. Renner, Z. Phys. 92, 172 (1934).
[53] Y. Fukumoto, H. Koizumi, K. Makoshi, Chem. Phys. Lett. 313, 283 (1999).
[54] D.R. Yarkony, Acc. Chem. Res. 31, 511 (1998).
[55] A.M. Mebel, M. Baer, S.H. Lin, J. Chem. Phys. 114, 5109 (2001).